




A new early diverging thalattosuchian (Crocodylomorpha) from the Early Jurassic (Pliensbachian) of Dorset, U.K. and implications for the origin and evolution of the group

Eric W. Wilberg, Pedro L. Godoy, Elizabeth F. Griffiths, Alan H. Turner & Roger B. J. Benson


To cite this article: Eric W. Wilberg, Pedro L. Godoy, Elizabeth F. Griffiths, Alan H. Turner & Roger B. J. Benson (2023): A new early diverging thalattosuchian (Crocodylomorpha) from the Early Jurassic (Pliensbachian) of Dorset, U.K. and implications for the origin and evolution of the group, *Journal of Vertebrate Paleontology*, DOI: [10.1080/02724634.2022.2161909](https://doi.org/10.1080/02724634.2022.2161909)

To link to this article: <https://doi.org/10.1080/02724634.2022.2161909>

 View supplementary material 

 Published online: 20 Jan 2023.




 Submit your article to this journal 

 Article views: 125

 View related articles 

 View Crossmark data 

A NEW EARLY DIVERGING THALATTOSUCHIAN (CROCODYLIFORMES) FROM THE EARLY JURASSIC (PLIENSCHACHIAN) OF DORSET, U.K. AND IMPLICATIONS FOR THE ORIGIN AND EVOLUTION OF THE GROUP

ERIC W. WILBERG, ^{*1} PEDRO L. GODOY, ^{1,2,3} ELIZABETH F. GRIFFITHS,⁴ ALAN H. TURNER,¹ and ROGER B. J. BENSON ⁴

¹Department of Anatomical Sciences, Stony Brook University, Stony Brook, New York 11794, U.S.A., eric.wilberg@stonybrook.edu;

²Department of Biology, University of São Paulo, Ribeirão Preto, São Paulo, 14040-901, Brazil, pedrolorenagodoy@gmail.com;

³Department of Zoology, Federal University of Paraná, Curitiba, Paraná 81531-980, Brazil;

⁴Department of Earth Sciences, University of Oxford, Oxford OX1 3AN, U.K.

ABSTRACT—Among archosaurs, thalattosuchian crocodylomorphs experienced the most extensive adaptations to the marine realm. Despite significant attention, the phylogenetic position of the group remains uncertain. Thalattosuchians are either the sister-group to Crocodyliformes, basal mesoeucrocodylians, or nest among longirostrine neosuchians. The earliest definite thalattosuchians are Toarcian, and already possess many synapomorphies of the group. All phylogenetic hypotheses imply a ghost lineage extending at least to the Sinemurian, and a lack of older or more plesiomorphic forms may contribute to the uncertain phylogenetic placement of the group. Here we describe a new species, *Turnersuchus hingleyae*, gen. et sp. nov., from the early Pliensbachian Belemnite Marl Member of the Charmouth Mudstone Formation (Dorset, U.K.). The specimen includes partially articulated cranial, mandibular, axial, and appendicular elements. It can be attributed to Thalattosuchia based on the following features: distinct fossa on the posterolateral corner of the squamosal; broad ventrolateral process of the otoccipital covering the dorsal surface of the quadrate; large supratemporal fenestrae lacking a flattened skull table; broadly exposed prootic; orbital process of quadrate lacking bony attachment with the braincase. This specimen represents the earliest thalattosuchian currently known from diagnostic material. Phylogenetic analyses of two published datasets recover *Turnersuchus* as the earliest diverging thalattosuchian, and sister to Teleosauroidea + Metriorhynchoidea. Bayesian tip-dating analyses suggest a Rhaetian or Sinemurian divergence of Thalattosuchia from other crocodylomorphs, depending on topology, with confidence intervals spanning from the Norian to the Pliensbachian. The new specimen extends the fossil record of Thalattosuchia, but the time-scaling analyses demonstrate that a significant ghost lineage remains.

<http://zoobank.org/urn:lsid:zoobank.org:pub:7BBDF9DB-AB15-476C-A41B-BAC65AE2709A>

SUPPLEMENTAL DATA—Supplemental materials are available for this article for free at www.tandfonline.com/UJVP.

Citation for this article: Wilberg, E. W., P. L. Godoy, E. F. Griffiths, A. H. Turner, and R. B. J. Benson. (2023) A new early diverging thalattosuchian (Crocodylomorpha) from the Early Jurassic (Pliensbachian) of Dorset, U.K. and implications for the origin and evolution of the group. *Journal of Vertebrate Paleontology*. Advance online publication. <https://doi.org/10.1080/02724634.2022.2161909>

INTRODUCTION

Thalattosuchian crocodylomorphs were prominent members of marine ecosystems from the Lower Jurassic through the Lower Cretaceous (Buffetaut, 1980, 1982; Vignaud, 1995; Hua & Buffetaut, 1997; Pierce et al., 2009a, b; Young et al., 2010, 2012; Wilberg, 2015a; Johnson et al., 2020a, b). They appear abruptly in the fossil record with high species richness, suggesting rapid diversification during the Toarcian. Seven species are currently known from this time period (*Plagiophthalmosuchus gracilirostris*; *Macrospondylus bollensis*; *Platysuchus multiscrobiculatus*; *Myrstriosaurus laurillardii*; an unnamed Chinese teleosauroid [IVPP V 10098]; *Magyarosuchus fitosi*; *Pelagosaurus typus*), across a wide geographic distribution. While most specimens are found in Europe (e.g., Jäger, 1828; Eudes-Deslongchamps,

1863–1869; Westphal, 1961, 1962; Duffin, 1979; Buffetaut, 1980; Benton & Taylor, 1984; Mueller-Töwe, 2006; Pierce & Benton, 2006; Ősi et al., 2018; Sachs et al., 2019), Toarcian specimens have also been reported from China (IVPP V 10098; Li, 1993), Argentina (Huene, 1927; Pol & Gasparini, 2007), and Madagascar (Buffetaut et al., 1981).

Older, but more fragmentary, specimens have been attributed to Thalattosuchia from the Sinemurian and Pliensbachian. These include partial metatarsals (MGHF 3601) from the Sinemurian of Chile (Thalattosuchia indet.; Chong Díaz and Gasparini, 1972; Gasparini et al., 2000) and two partial vertebrae from the upper Sinemurian of France (Teleosauridae indet.; Huene & Maubeuge, 1954). Additionally, a block including osteoderms, a partial femur, and other fragments (NHMUK PV R 4143) has been reported from the Kota Formation of India (Owen, 1852), though it is unclear whether this specimen is Pliensbachian or Toarcian in age. While some or all of these specimens may belong to Thalattosuchia, none possess any thalattosuchian apomorphies, so their validity as early records of the group cannot be confirmed.

There are reasons to expect a pre-Toarcian record of Thalattosuchia. Firstly, because thalattosuchian diversity was relatively

*Corresponding author

This article has been corrected with minor changes. These changes do not impact the academic content of the article.

Color versions of one or more of the figures in the article can be found online at www.tandfonline.com/ujvp.

high already by the early Toarcian, as evidenced by deposits of western Europe (e.g., four species from Posidonia Shale; Mueller-Töwe, 2006). Secondly, because the group had achieved a nearly global distribution by this time (Europe, Argentina, Madagascar, China) implying an earlier unsampled history. And finally, because most recent phylogenies require a ghost lineage leading to Thalattosuchia minimally originating by the Sinemurian (e.g., Tykoski et al., 2002; Jouve, 2009; Pol & Gasparini, 2009; Andrade et al., 2011; Pol et al., 2014; Turner, 2015; Turner & Pritchard, 2015; Leardi et al., 2017; Martínez et al., 2018) or the Late Triassic (e.g., Wilberg, 2015a, b, 2017; Young et al., 2017; Foffa et al., 2018; Martin et al., 2019; Wilberg et al., 2019; Melstrom et al., 2022).

In addition to these temporal uncertainties, the phylogenetic position of Thalattosuchia within Crocodylomorpha also remains somewhat contentious, despite decades of phylogenetic analyses. This issue has been termed the “longirostrine problem” (Clark, 1994; Jouve, 2006; Pol & Gasparini, 2009; Wilberg, 2015b). Thalattosuchia is consistently recovered in one of three positions depending on dataset and taxon sample:

- (1) As sister-group to Crocodyliformes (Jouve, 2009; Pol & Gasparini, 2009; Wilberg, 2015a, b, 2017; Young et al., 2017; Foffa et al., 2018; Wilberg et al., 2019).
- (2) As early diverging mesoeucrocodylians (e.g., Sereno et al., 2001, 2003; Larsson & Sues, 2007; Sereno & Larsson, 2009; Young et al., 2012, 2020, 2021; Montefeltro et al., 2013; Johnson et al., 2020b; Herrera et al., 2021).
- (3) Within Neosuchia, sister to Tethysuchia (e.g., Clark, 1994; Wu et al., 1997, 2001; Brochu et al., 2002; Jouve et al., 2006; Jouve, 2009; Pol & Gasparini, 2009; Turner & Sertich, 2010; Andrade et al., 2011; Pol et al., 2014; Leardi et al., 2015).

Contributing to this issue is the highly autapomorphic nature of Thalattosuchia, placing them on a long phylogenetic branch in terms of morphological character state changes. Even the earliest known thalattosuchians already possess autapomorphies of the group and the lack of more plesiomorphic forms likely hinders the phylogenetic placement of the group within Crocodylomorpha. Given the long ghost lineage implied for Thalattosuchia in most topologies, more plesiomorphic forms could potentially be found in pre-Toarcian sediments.

Here we describe new cranial and postcranial material of a marine crocodylomorph from the early Pliensbachian (c. 190 Ma) Belemnite Marl Member of the Charmouth Mudstone Formation (Dorset, U.K.). This represents the earliest diagnostic material of Thalattosuchia reported to date. Investigation of its morphology and phylogenetic relationships will help elucidate the plesiomorphic condition for the clade. Its early occurrence may also improve our understanding of the divergence time for Thalattosuchia.

Institutional Abbreviations—**BRLSI**, Bath Royal Literary and Scientific Institution, Bath, United Kingdom; **BRSMG**, Bristol City Museum and Art Gallery, Bristol, United Kingdom; **FMNH**, Field Museum of Natural History, Chicago, Illinois, U.S.A.; **IVPP**, Institute of Vertebrate Paleontology and Paleoanthropology, Beijing, China; **LYMPH**, Lyme Regis Museum, Lyme Regis, United Kingdom; **MACN-RN**, Museo Argentino de Ciencias Naturales (Rio Negro Collection), Buenos Aires, Argentina; **MB**, Museum für Naturkunde, Berlin, Germany; **MCZ**, Museum of Comparative Zoology, Harvard University, Cambridge, Massachusetts, U.S.A.; **MLP**, Museo de La Plata, La Plata, Argentina; **MNHN**, Muséum National d’Histoire Naturelle, Paris, France; **MPV**, Musée paléontologique de Villers-sur-Mer, Paléospace l’Odyssee, Villers-sur-Mer, France; **MTM**, Hungarian Natural History Museum, Budapest, Hungary; **NHMUK**, Natural History Museum, London, United Kingdom;

PRC, Palaeontological Research and Education Centre, Maha Sarakham University, Maha Sarakham, Thailand; **RMH**, Roemer und Pelizaeus Museum, Hildesheim, Germany; **SMNS**, Staatliches Museum für Naturkunde, Stuttgart, Baden-Württemberg, Germany; **SNSB-BSPG**, Bayerische Staatssammlung für Paläontologie und Geologie, Munich, Germany; **UH**, Urwelt Museum Hauff, Holzmaden, Germany; **UOMNH**, University of Oregon Museum of Natural and Cultural History, Eugene, Oregon, U.S.A.

GEOLOGIC SETTING

LYMPH 2021/45 was recovered from the Belemnite Marls Member of the Charmouth Mudstone Formation (Barton et al., 2011) on the coast west of Charmouth (E. Hingley, pers. comm.). It occurred in eroded material that may have originated from Bed 107, 108, 109 or nearby (bed numbers from Lang et al., 1928) (P. Davis, pers. comm.). It is therefore Pliensbachian in age, representing the *Uptonia jamesoni* chronozone, and possibly (depending on the accuracy of bed-level provenance data) *Phricodoceras taylori* subchronozone and PbH2 Taylori horizon (chronostratigraphy after Page, 2010).

MATERIALS AND METHODS

Micro-computed Tomography

The main block of LYMPH 2021/45 initially comprised the portions now labeled as ‘block 1’ and ‘block 3’ (Fig. 1). We used micro-CT scanning to establish the distribution of bone in the main block, seeking to reduce overall block size to achieve higher scan quality (i.e., reduced noise, increased resolution and increased contrast between bone and matrix). Our initial pilot scan indicated that the block could be prepared into two smaller blocks. We re-scanned these blocks, from which individual bones were then segmented by E.F.G. using Mimics version 19.0 (Materialise, Leuven). Scans were carried out using a Nikon Metrology XT H 225 ST micro-CT scanner in the XTM Facility, Palaeobiology Research Group, University of Bristol. Scan image volumes, 3D models, and metadata including scan settings are available at www.morphosource.org/projects/00000C757.

Phylogenetic Analyses

To determine the phylogenetic position of *Turnersuchus hingleyae* we performed two new analyses. The first is based on the dataset of Wilberg et al. (2019), which is the most recent version of the matrix originally presented by Wilberg, 2015b. Taxon sampling was increased to 105 operational taxonomic units (OTUs) and character sampling increased to 410 (77 of which could be scored for *T. hingleyae*). This dataset includes 33 thalattosuchian OTUs excluding *T. hingleyae*. The second analysis is based on the dataset of Herrera et al. (2021), which is one of the most recent versions of the character matrix commonly referred to as the “H+Y matrix” (or the “Hastings+Young matrix”), originally presented by Young et al. (2017), but later modified by Ristevski et al. (2018), Ósi et al. (2018), and Aiglstorfer et al. (2020). Our version of this dataset differs from that of Herrera et al. (2021) only by the addition of the new taxon (*T. hingleyae*) and minor rescaling of some characters based on firsthand observation, particularly for *Peipehsuchus telaeorhinus*. As in prior iterations of this matrix, *Congosaurus bequaerti*, *Crocodylus acutus*, *Cr. intermedius*, *Cr. mindorensis*, *Cr. moreletti*, *Cr. rhombifer*, *Cr. suchus*, and the “Swiss rhaecosaurin” were unstable OTUs and were excluded from the analysis. The resulting dataset includes 169 OTUs scored for 519 characters (80 of which could be scored for *T. hingleyae*). Excluding *T. hingleyae*, 78 of the OTUs are thalattosuchians.

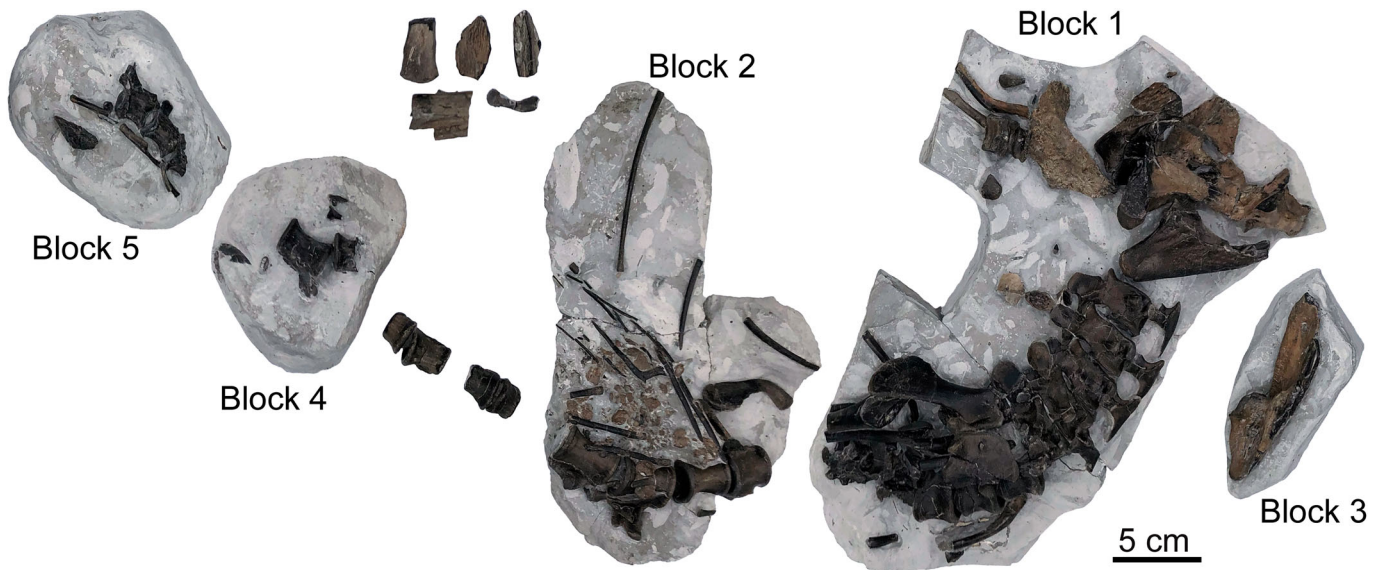


FIGURE 1. Preserved material of *Turnersuchus hingleyae* gen. et sp. nov. (LYMPH 2021/45) including five main blocks and isolated elements.

The phylogenetic data matrices are available on MorphoBank (O’Leary & Kaufman, 2011, 2012) at <http://morphobank.org/permalink/?P4271>. Details of the phylogenetic analysis methodology, character descriptions, and materials referenced for character scoring are available in the Supplementary Materials. The datasets were analyzed in TNT v1.5 (Goloboff & Catalano, 2016) under equally weighted parsimony. A heuristic search included 1000 replicates of Wagner trees using random addition sequences followed by TBR (tree bisection and reconnection) branch swapping holding 10 trees per replication. The shortest trees obtained from these replicates were subjected to a final round of TBR branch swapping to ensure all minimum length trees were discovered. Zero-length branches were collapsed if they lacked support under any of the minimal length trees (Rule 1 of Coddington & Scharff, 1994). The strict consensus trees were used to report the results of each analysis.

Time-calibration of the Topologies

We performed Bayesian analyses to time-calibrate the topologies that resulted from the parsimony analyses. The strict consensus trees obtained from both datasets (Wilberg et al., 2019 and Herrera et al., 2021) were used as topological constraints for time-calibration analyses, with the only difference that, in the strict consensus obtained from the Herrera et al. (2021) dataset, we manually changed the position of *Eopneumatosuchus colberti*, from sister to Thalattosuchia to sister to *Protosuchus* (within Protosuchidae), following a recent reassessment of the taxon (Melstrom et al., 2022). Bayesian tip-dating analyses were performed under a fossilized birth–death (FBD) model (Stadler, 2010; Ronquist et al., 2012a; Heath et al., 2014; Zhang et al., 2016), using an empty character matrix created with the createMrBayesTipdatingNexus function within the paleotree R package (Bapst, 2012), which follows the recommendations within Matzke and Wright (2016). Uniform priors were placed on taxon ages, with the age of extant taxa fixed to 0 and the age range of extinct taxa obtained from the literature. A uniform prior was also placed on the age root of the entire tree, constraining it between 245 and 260 Myr ago (given that a crocodylomorph origin older than the Early Triassic is unlikely (Turner et al., 2017; Ezcurra & Butler, 2018)). For each dataset,

two independent MCMC runs were performed in MrBayes version 3.2.6 (Ronquist et al., 2012b), with four chains of 35,000,000 generations each, sampling every 1,000 generations. Convergence was assessed using potential scale reduction factor (PSRF; values approaching 1.0) and average standard deviation of split frequencies (values below 0.01). After the runs converged, 25% of sampled trees were discarded as burn-in. For reporting the results, only the majority rule consensus (MRC) tree was used.

SYSTEMATIC PALEONTOLOGY

CROCODYLOMORPHA Hay, 1930, sensu Nesbitt, 2011
 THALATTOSUCHIA Fraas, 1901, sensu Young, and
 Andrade, 2009
TURNERSUCHUS, gen. nov.

Type Species—*Turnersuchus hingleyae*

Etymology—After Paul Turner, who discovered and donated the initial block of the specimen and “suchus,” from the Latinized form of “soukhos,” Greek for crocodile.

Diagnosis—As for the type species.

TURNERSUCHUS HINGLEYAE sp. nov.
 (Figs. 1–9)

Holotype—LYMPH 2021/45, partial skull, partial mandible, cervical and dorsal vertebrae in articulation and isolated caudal vertebrae, cervical and dorsal ribs, right pectoral girdle (right scapula and partial right coracoid), partial right humerus, ulna, partial tibia, one dorsal osteoderm.

Etymology—After Elizabeth “Lizzie” Hingley, who discovered additional material and prepared the specimen.

Locality and Horizon—*Uptonia jamesoni* chronozone of the Belemnite Marl Member of the Charmouth Mudstone (Lower Jurassic, Pliensbachian). Recovered as eroded material adjacent to the beach approximately one kilometer west of the Charmouth Heritage Coast Centre, Charmouth, Bridport DT6 6LL, U.K.

Diagnosis—Thalattosuchian crocodylomorph with the following unique combination of characters (autapomorphies indicated

by an asterisk*): dorsally directed prootic peg along suture with parietal*; enlarged median pharyngeal foramen*; quadrate broadly separated from trigeminal foramen*; tall, vertically oriented squamosal occipital surface*; posterolateral corner of supratemporal fossa well posterior to occipital condyle; squamosal fossa facing slightly ventrally*; scapula with anterior margin more strongly concave than posterior margin. Differs from *Pelagosaurus* in: posterior margin of the supratemporal fenestra more posterolaterally inclined; supratemporal fossa extending further posterolaterally; squamosal fossa oriented slightly ventrally; tall, vertical occipital surface of squamosal; scapula with relatively straight posterior margin; ulna broader proximally, with more strongly curved shaft. Differs from *Plagiophthalmosuchus* in: tall, vertical occipital surface of squamosal; broader intertemporal bar (at least anteriorly); anteroposteriorly shorter retroarticular process lacking a distinct ridge on the dorsal surface.

DESCRIPTION

General Description

The specimen is relatively three-dimensionally preserved and in partial articulation, with elements preserved in five separate blocks (Fig. 1) that were recovered over a period of 15 months (May 2017–July 2018), due to gradual weathering, from the type locality. Preserved cranial material consists primarily of elements from the posterior right side including much of the braincase and occipital region, all of which are preserved in the main block (or block 1). Mandibular fragments are preserved in blocks 1 and 3 (which was prepared away from block 1) and include both retroarticular processes and small isolated fragments of both the dentaries and angulars. The axial and appendicular elements are preserved in four of the blocks, with the cervical and dorsal vertebrae in blocks 1 and 2 preserved in articulation. Blocks 4 and 5 preserve caudal vertebrae. Preserved appendicular elements include the right scapula, coracoid, and humerus (block 1), right ulna (block 2), and an isolated long bone fragment (possibly a distal tibia). Numerous ribs and rib fragments are preserved among the blocks, as well as at least one dorsal osteoderm (block 1). Additional photographs of all blocks and isolated elements are available at www.morphobank.org/permalink/?P4271.

Major Cranial Openings

Choana—The choana itself is not preserved, but the preserved portion of the pterygoid shows that it opened into a broad depression on the ventral surface of the pterygoid (Fig. 2). It terminates posteriorly at a short, gently curving (concave anteriorly) ridge, similar to that of *Pelagosaurus typus* (NHMUK PV OR 32599; Mueller-Töwe, 2006), but differing from the shallower depression marking the posterior margin of the choana of some other thalattosuchians (e.g., *Teleosaurus*; Jouve, 2009). The relatively posterior position of this posterior margin of the choana suggests a more extensive secondary palate than present in “sphenosuchian” grade basal crocodylomorphs and protosuchids (Dollman & Choiniere, 2022).

Supratemporal Fenestra—Much of the right supratemporal fenestra (STF) is preserved, lacking its anterior and anterolateral margins (Fig. 2). The posterior portion of the intertemporal bar is also incomplete. The STF is large with a well-developed fossa posteriorly (and somewhat medially). The medial margin is formed by the frontal and parietal, the posterior margin by the parietal and squamosal, and the lateral margin by the squamosal and postorbital. The posterior margin is inclined posterolaterally at approximately 50°. The posterolateral corner greatly exceeds the occipital condyle posteriorly, though this might be

exaggerated by the slight postmortem displacement of some of the cranial elements. This posterolateral inclination of the posterior margin of the STF is greater than that of *Pelagosaurus* (~65°; NHMUK PV OR 32599), or *Plagiophthalmosuchus* (~65°; NHMUK PV OR 15500). Lack of preservation of the anterior portion of the STF prevents detailed description of its shape, but based on the preserved portions, the STF is anteroposteriorly longer than mediolaterally wide.

Temporo-orbital Foramen—The temporo-orbital foramen is visible in dorsal view on the posterior wall of the supratemporal fossa (Fig. 2). The squamosal forms its lateral and short parts of the dorsal and ventral margins. The parietal forms the remainder of the dorsal border. The prootic appears to form the medial and remainder of the ventral border, potentially excluding the quadrate from the margin of the foramen. However, sutures are difficult to discern in this region.

Cranioquadrate Canal—Part of the right cranioquadrate canal is preserved (Fig. 3). It is positioned laterally on the occipital surface, between the paroccipital and inferolateral processes of the otoccipital. The otoccipital forms the dorsal, medial, and inferior borders. As preserved, the canal is open laterally. However, the lateral surface of the quadrate and inferior portion of the squamosal fossa are damaged. Thus, it is possible that the canal was fully enclosed by some combination of these bones.

Foramen Magnum—The inferior and right lateral borders of the foramen magnum are preserved (Fig. 3). The otoccipital forms the lateral and a small part of the inferior borders. The basioccipital forms the remainder of the inferior border. The superior border is not preserved so it is unclear whether the supraoccipital would have contributed to the superior border.

Bones of the Skull

Frontal—Most of the frontal is missing from the specimen (Figs. 2, 3). The wider, anterior-most preserved portion of the intertemporal bar likely preserves the posterior-most part of the posterior process of the frontal. However, the suture with the parietal is not obvious in the scan. The dorsal surface of this portion of the intertemporal bar preserves a few anteroposteriorly elongate oval pits, suggesting ornamentation of this element similar to that of the postorbital and squamosal.

Parietal—The parietal is a single, fused element in LYMPH 2021/45, though only portions of it are preserved (Figs. 2, 3). The parietal is Y-shaped, with an anterior process and right and left posterolateral processes (of which only the right is preserved). The anterior process articulates with the frontal anteriorly, the laterosphenoid, and prootic inferolaterally. The parietal makes up most of the intertemporal bar, though uncertainty of the position of the frontal suture and damage to the posterior region of the bar prevents giving exact proportions. The surface bone is missing on the posterior region of the intertemporal bar, so it is unclear if a narrow sagittal crest would have been present as in most metriorhynchids, or if the intertemporal bar would have maintained its width throughout as in *Pelagosaurus* (NHMUK PV OR 32599; Mueller-Töwe, 2006) or *Teleosaurus* (Jouve, 2009).

The posterolateral process of the parietal articulates with the squamosal laterally and the otoccipital posteriorly. At the junction of the posterolateral processes, the parietal would have articulated with the supraoccipital, a small portion of which may be preserved, though its suture with the parietal is unclear. The parietal contributes to the occipital surface, though the medial portion is missing. The parietal occipital surface is slightly sloped posteroventrally, differing from the more vertical orientation of the squamosal occipital surface.

Postorbital—The posterior portion of the right postorbital is preserved in articulation with the squamosal (Figs. 2, 3). The

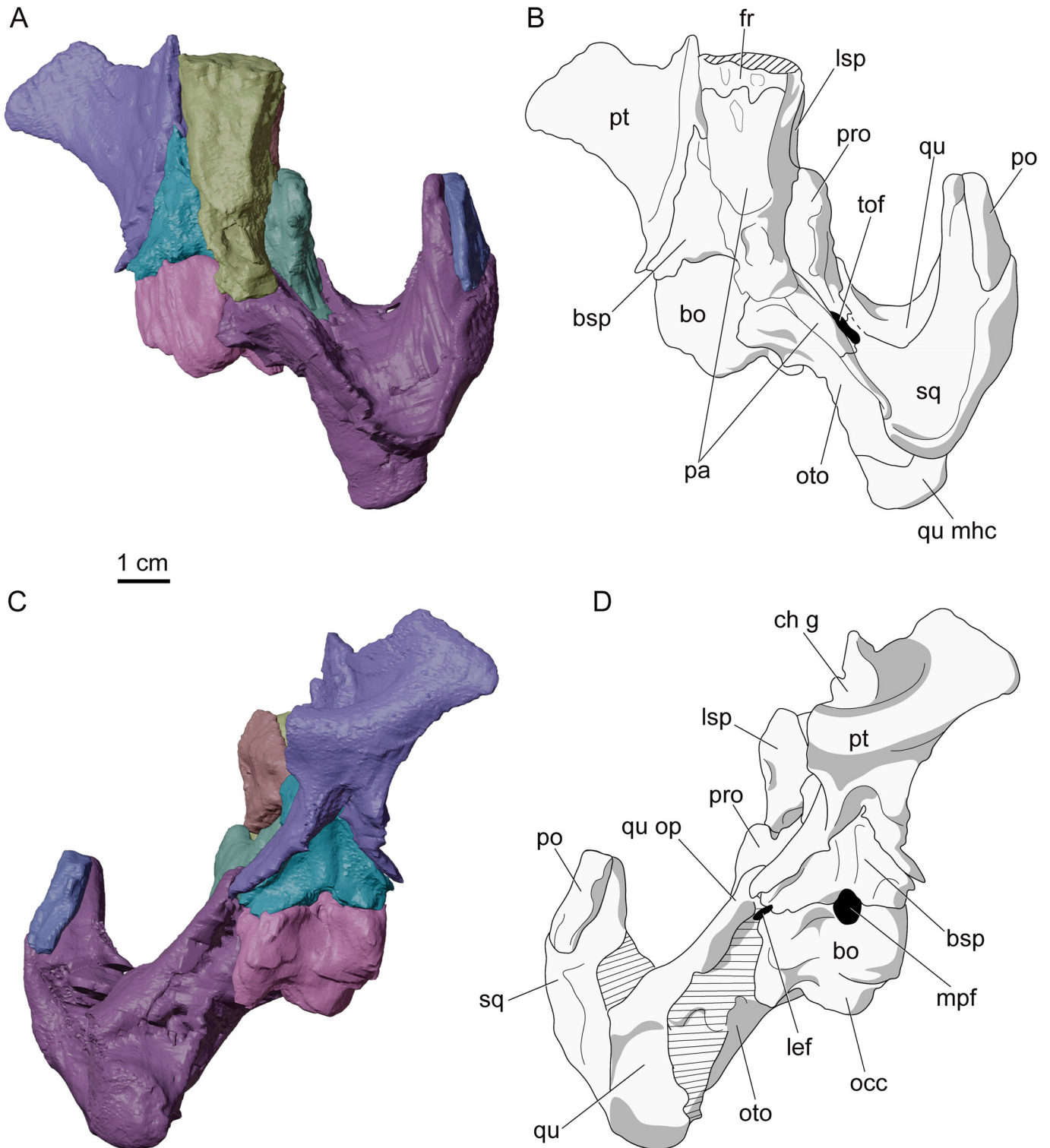


FIGURE 2. Skull of *Turnersuchus hingleyae* gen. et sp. nov. (LYMPH 2021/45). **A**, digital model in dorsal view; **B**, line interpretation of same; **C**, digital model in ventral view; **D**, line interpretation of same. **Abbreviations:** **bo**, basioccipital; **bsp**, basisphenoid; **ch g**, choanal groove; **fr**, frontal; **lef**, lateral Eustachian foramen; **lsp**, laterosphenoid; **mpf**, median pharyngeal foramen; **occ**, occipital condyle; **oto**, otocipital; **pa**, parietal; **po**, postorbital; **pro**, prootic; **pt**, pterygoid; **qu**, quadrate; **qu mhc**, quadrate medial hemicondyle; **qu op**, quadrate orbital process; **sq**, squamosal; **tof**, temporo-orbital foramen.

preserved portion is dorsoventrally tall and mediolaterally narrow. Its lateral surface is ornamented with distinct pits, some of which are elongated longitudinally into short grooves.

The presence of ornamentation on the lateral temporal bar is uncommon among thalattosuchians, but is shared with *Pelagosaurus* (NHMUK PV OR 32599; Mueller-Töwe, 2006),

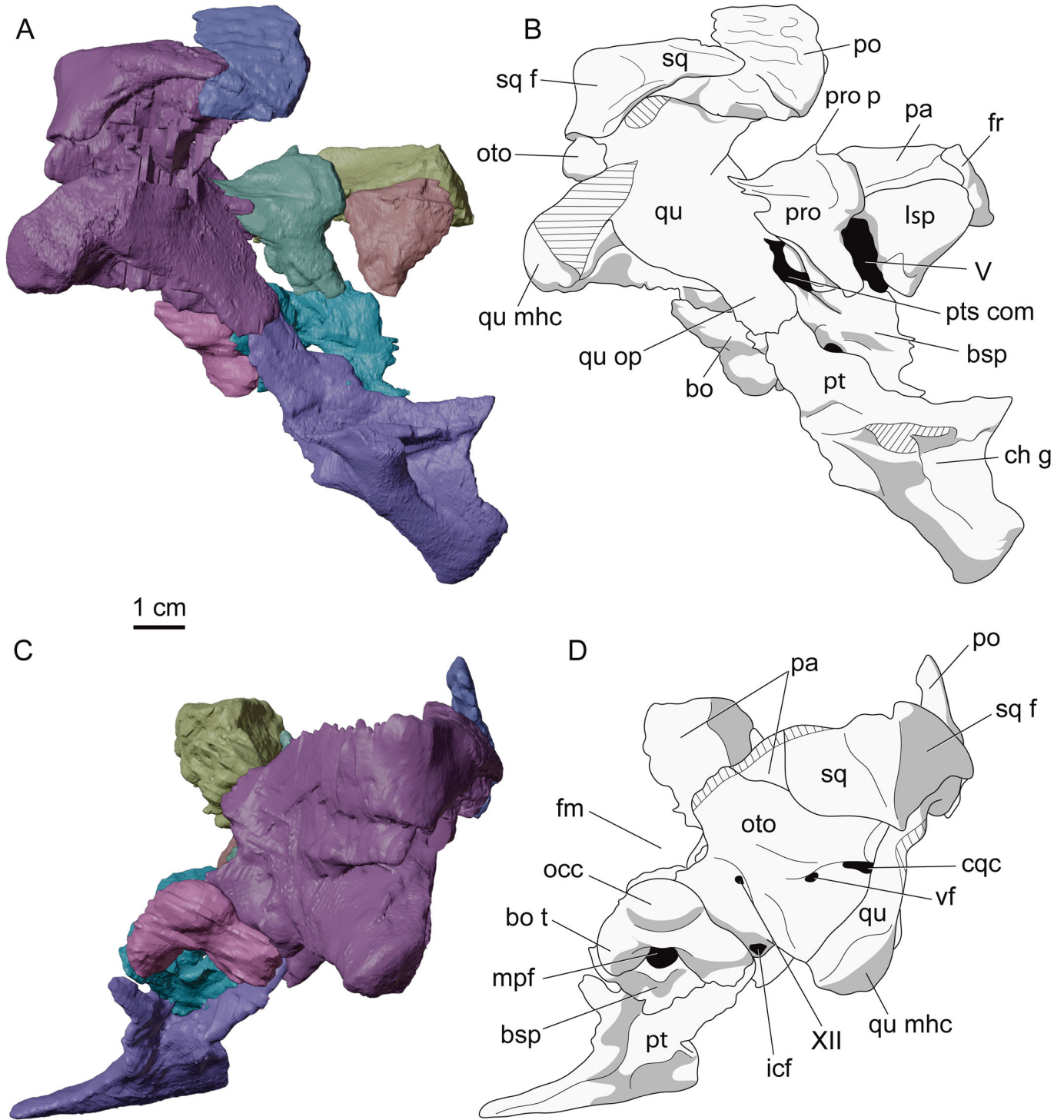


FIGURE 3. Skull of *Turnersuchus hingleyae* gen. et sp. nov. (LYMPH 2021/45). **A**, digital model in ventrolateral view; **B**, line interpretation of same; **C**, digital model in occipital view; **D**, line interpretation of same. **Abbreviations:** **bo**, basioccipital; **bo t**, basioccipital tuberosity; **bsp**, basisphenoid; **ch g**, choanal groove; **cqc**, cranioquadrate canal; **fm**, foramen magnum; **fr**, frontal; **icf**, internal carotid foramen; **lsp**, laterosphenoid; **mpf**, median pharyngeal foramen; **occ**, occipital condyle; **oto**, otoccipital; **pa**, parietal; **po**, postorbital; **pro**, prootic; **pro p**, prootic peg; **pt**, pterygoid; **pts com**, communication with paratympanic sinus; **qu**, quadrate; **qu mhc**, quadrate medial hemicondyle; **qu op**, quadrate orbital process; **sq**, squamosal; **sq f**, squamosal fossa; **V**, trigeminal foramen; **vf**, vagus foramen; **XII**, hypoglossal foramen.

Platysuchus multiscrobiculatus (SMNS 9930; Mueller-Töwe, 2006), and to a lesser extent *Plagiophthalmosuchus gracilirostris* (NHMUK PV R 757). An anteroposteriorly directed ridge runs near the ventral margin of the bone, separating a narrow

unornamented flange from the ornamented area above similar to *Pelagosaurus typus* (NHMUK PV OR 32599).

The postorbital articulates posteriorly with the squamosal at a v-shaped suture, with an anterior projection of the squamosal

dividing the posterior margin of the postorbital into two posterior processes, as in most thalattosuchians (e.g., *Teleosaurus cadomensis* [Jouve, 2009]; *Indinosuchus potamosiamensis* [Martin et al., 2019]; *Pelagosaurus* [NHMUK PV OR 32599]). The dorsal process is much larger than the ventral process and articulates only with the squamosal. The ventral process is narrower, and articulates with the squamosal and the dorsolateral process of the quadrate, anterior to the external acoustic meatus. The dorsal surface of the postorbital narrows to a ridge, continuous with the dorsal surface of the squamosal (postorbital-squamosal ridge sensu Young et al., 2013).

Squamosal—The right squamosal is nearly complete (Figs. 2, 3). The bone is v-shaped, with its anterior and medial processes forming an acute angle (~60°) similar to *Pelagosaurus typus* (NHMUK PV OR 32599), *Opisuchus meieri* (Aiglstorfer et al., 2020), and *Plagiophthalmosuchus gracilirostris* (NHMUK PV OR 15500), but differing from the condition in many teleosaurids (e.g., *Teleosaurus* [Jouve, 2009]; *Indosinosuchus* [Martin et al., 2019]; *Macrospandylus* [Wilberg et al., 2022]) and most metriorhynchids (e.g., *Torvoneustes* [Young et al., 2013]; and *Purransaurus* [Herrera et al., 2015]) where the angle is closer to 90°. It articulates anteriorly and laterally with the postorbital, ventrally with the quadrate, posteriorly with the otoccipital and medially with the parietal. The supratemporal fossa extends posterolaterally along the squamosal, forming narrow, elevated ridges along the dorsal surface of the anterior and medial processes. The squamosal articulates with the parietal dorsal to the temporo-orbital foramen, just medial to its lateral border. The squamosal forms the lateral and ventrolateral borders of the temporo-orbital foramen, and contributes slightly to the dorsal border. It is unclear whether the process of the squamosal forming the ventrolateral border of the temporo-orbital foramen would have contacted the prootic medially (excluding the quadrate from the margin of the opening) as in most metriorhynchoids and some teleosauroids (e.g., *Macrospandylus bollenensis* [MCZ PVRA-1063]; Wilberg et al., 2022), or whether the quadrate would have contributed to the ventral margin as in *Teleosaurus* (Jouve, 2009) and *Indosinosuchus* (Martin et al., 2019).

The lateral surface of the anterior process of the squamosal is ornamented with closely spaced deep pits, similar to the postorbital. The posterolateral surface is smooth and gently concave, forming a shallow trapezoidal squamosal fossa (sensu Wilberg et al., 2022), although the ventral-most portion is missing. The shape of the fossa is similar to *Pelagosaurus* (NHMUK PV OR 32599), but differs from the dorsoventrally elongate fossa of *Macrospandylus bollenensis* (MCZ PVRA-1063; Wilberg et al., 2022). Unlike other known thalattosuchians, the squamosal fossa of LYMPH 2021/45 appears to be directed slightly ventrally, rather than dorsally. The squamosal fossa lies posterodorsal to the external otic aperture.

The occipital surface of the medial process of the squamosal is dorsoventrally taller than other known thalattosuchians and articulates ventrally with the paroccipital process of the otoccipital and medially with the occipital surface of the parietal. The occipital surface of the squamosal is approximately twice the dorsoventral height of the distal end of the paroccipital process, though the sutures in this region are difficult to make out.

Quadrate—Most of the right quadrate is preserved (Figs. 2, 3), lacking only the lateral hemicondyle. However, sutures with the surrounding bones are difficult to delineate and artifacts in the scan obscure detail in the otic region. The quadrate articulates with the squamosal anterodorsally, the otoccipital posterodorsally, the prootic anteromedially, the basisphenoid and pterygoid ventromedially. The quadrate body is inclined posterovertrally, positioning the medial hemicondyle ventral to the occipital condyle, approximately in line with the ventral margin of the basal tubera as in *Pelagosaurus* (NHMUK PV OR 32599;

Mueller-Töwe, 2006). Its posterodorsal surface is broadly overlapped by the ventrolateral process of the otoccipital. The medial hemicondyle is ventromedially inclined, with its main axis oriented approximately 45° from horizontal. The ventral surface of the quadrate body is either damaged anterior to the medial hemicondyle, or artifacts in the scan prevent segmenting of its ventral surface.

The dorsolateral process of the quadrate is preserved, but the presence of several highly absorbing objects in the scan makes this region difficult to interpret due to beam hardening artifacts. As in other thalattosuchians, the quadrate articulates with the ventral surface of the squamosal, sending a thin otic lamina posteriorly to form the roof of the external otic aperture, excluding the squamosal from its margin. The dorsolateral process potentially articulated with the posteroventral surface of the postorbital, but as the sutures in this region are unclear, this cannot be confirmed.

The dorsal primary head of the quadrate contacts the lateral wall of the braincase, but these articulations appear narrower than in other thalattosuchians or crocodyliforms. Anteromedially, it is sutured to the ventral margin of the medial process of the squamosal and has an anteroventrally sloping suture with the prootic, contributing to the posteroventral wall of the supratemporal fossa. This contact with the prootic is shorter than in other thalattosuchians, where the quadrate extends anteriorly along the prootic to reach or nearly reach the trigeminal foramen. In *Turnersuchus*, the quadrate is broadly separated from the trigeminal foramen by the prootic and basisphenoid, unlike crocodyliforms generally (Clark, 1994).

The pterygoid process of the quadrate has a short, obliquely oriented suture with the posterolateral lamina (quadrate process) of the pterygoid. Extending anteriorly is a short, squared orbital process. The orbital process of *Turnersuchus* is similar in shape to *Pelagosaurus*, but oriented more ventrally along the braincase. The orbital process primarily articulates with the pterygoid and basisphenoid (reminiscent of *Sphenosuchus acutus* [Walker, 1990], but with a very different pterygoid morphology). This differs from other thalattosuchians in which the orbital process is more anteriorly oriented, articulating with the laterosphenoid in addition to the pterygoid and basisphenoid (e.g., *Macrospandylus*; Wilberg et al., 2022). As in other thalattosuchians (e.g., *Pelagosaurus* [NHMUK PV OR 32599]; *Plagiophthalmosuchus* cf. *gracilirostris* [NHMUK PV OR 33095; Brusatte et al., 2016]; *Cricosaurus araucanensis* [Herrera et al., 2018]; *Metriorhynchus* cf. *westerni* [Fernández et al., 2011]; *Macrospandylus bollenensis* [MCZ PVRA-1063]; *Machimosaurus buffetauti* [SMNS 91415]; *Teleosaurus cadomensis* [Jouve, 2009]), the orbital process lacks bony attachment to the pterygoid, basisphenoid, or laterosphenoid anteromedially. The short length and more ventral orientation of the orbital process of the quadrate in *Turnersuchus* results in a very broad separation from the laterosphenoid.

Laterosphenoid—The posterior portion of the right laterosphenoid is preserved (Figs. 2, 3). It articulates with the frontal anterodorsally, the parietal posterodorsally, the prootic posteriorly, and the basisphenoid ventrally. The laterosphenoid has been slightly displaced from the adjacent bones. Because the laterosphenoid is not preserved in articulation with the prootic, it is unclear whether this suture formed a raised ridge dorsal to the trigeminal foramen as in most thalattosuchians (e.g., *Pelagosaurus* [NHMUK PV OR 32599]; *Plagiophthalmosuchus* cf. *gracilirostris* [NHMUK PV OR 33095; Brusatte et al., 2016]; *Suchodus brachyrhynchus* [NUMHK PV R 3700]). When a ridge is present, it divides the supratemporal fossa into posterior and anterior fossae interpreted as the insertions for *M. adductor mandibulae externus profundus* and *M. pseudotemporalis superficialis*, respectively (Holliday & Witmer, 2009). The lateral surface of the preserved portion is vertical, becoming somewhat

ventrolaterally oriented anteriorly. The laterosphenoid forms the anterior margin of the trigeminal foramen.

Prootic—The right prootic is nearly complete (Figs. 2, 3). It is triangular in dorsal view and broadly exposed as in other thalattosuchians and non-crocodyliform crocodylomorphs (Clark, 1994). It articulates with the laterosphenoid anteriorly (though these bones have been slightly displaced), the parietal dorsally and posteriorly, the basisphenoid ventrally, and the quadrate posterolaterally. A small, dorsally directed peg is present along its suture with the parietal. A corresponding shallow notch on the lateral surface of the parietal intertemporal bar would have articulated with this peg. This dorsal prootic peg appears autapomorphic for LYMPH 2021/45. The prootic forms the ventral margin of the temporo-orbital foramen and potentially contacts the squamosal in this region. It forms the dorsal, posterior, and ventral margins of the dorsoventrally elongate trigeminal foramen. The dorsoventral elongation of the trigeminal foramen is similar to *Pelagosaurus* (NHMUK PV OR 32599; Holliday & Witmer, 2009), though *Turnersuchus* lacks the distinct constriction near the midpoint demarcating exit points for the root of the trigeminal and the rostral middle cerebral vein (Herrera, 2015). This shape differs from *Plagiophthalmosuchus* cf. *gracilirostris* (Brusatte et al., 2016) and most teleosauroids in which the foramen is more circular. In lateral view a broad lamina projects ventrally, immediately posterior to the trigeminal foramen (and forming its posterior border). This ventral lamina contacts the laterosphenoid anteroventrally and the basisphenoid posteroventrally, near the dorsal margin of the orbital process of the quadrate. This appears similar to the morphology of *Pelagosaurus* (BRLSI M1413; visible in the CT model by Ballell et al., 2019), where this broad process divides the trigeminal foramen from a lateral communication with the paratympanic sinus. However, it differs from the narrow lamina present in the teleosauroids *Macrospondylus bollensis* (MCZ VPRA-1063), *Machimosaurus buffetauti* (SMNS 91415), and *Proexochokefalos heberti* (MNHN 1890-13; Wilberg et al., 2022).

Otoccipital—The opisthotic and exoccipital are fused into a single otoccipital. Much of the right otoccipital is preserved, though its sutures with the quadrate, squamosal, and parietal are difficult to discern in the CT data (Figs. 2, 3). It articulates with the parietal dorsally, the squamosal dorsolaterally, the quadrate ventrolaterally, and the basioccipital and basisphenoid ventromedially. It forms the ventrolateral, lateral, and dorsolateral margin of the foramen magnum. The dorsal margin is incomplete, so it is not clear whether it contacted the left otoccipital dorsal to the foramen magnum, or whether the supraoccipital interposed between them.

The paroccipital process is well developed, and extends laterally to the lateral margin of the occipital surface. It is relatively vertical across its occipital surface, with its lateral half becoming slightly posteroventrally sloped. This lateral terminus ends just inferior to the broken inferior surface of the squamosal fossa. In other thalattosuchians (e.g., *Macrospondylus bollensis* [MCZ VPRA-1063; Wilberg et al., 2022]; *Pelagosaurus typus* [NHMUK PV OR 32599]; *Torvoneustes coryphaeus* [Young et al., 2013]), the lateral tip of the paroccipital process articulates with a concavity on the squamosal adjacent to the squamosal fossa. It is possible a similar configuration was present in LYMPH 2021/45, but damage to the squamosal fossa makes this uncertain.

Like other thalattosuchians, *Turnersuchus* possesses a broad ventrolateral flange of the otoccipital that broadly covers the dorsal surface of the quadrate body. A broad ventrolateral flange of the otoccipital is also present in protosuchids, though less developed than in thalattosuchians (Clark, 1994; Pol & Gasparini, 2009). Laterally, the ventrolateral flange ends slightly medial to the lateral end of the paroccipital process similar to *Cricosaurus araucanensis* (Herrera et al., 2018). This differs

from *Pelagosaurus* (NHMUK PV OR 32599), *Macrospondylus bollensis* (MCZ VPRA-1063), and *Cricosaurus rauhuti* (SNSB-BSPG 1973 I 195; Herrera et al., 2021) in which the ventrolateral flange exceeds the paroccipital process laterally.

Typically, a number of foramina pierce the otoccipital. No canals were traceable on the scan, but some of the foramina are apparent as depressions on the occipital surface. A depression lateral to the occipital condyle and approximately in line with the floor of the foramen magnum likely represents the hypoglossal foramen. A short distance ventrolaterally, near the articulation with the basioccipital tuber lies a circular depression potentially representing the internal carotid foramen. Unfortunately, given the preservation, it is difficult to determine whether it is enlarged as in other thalattosuchians. Located lateral to the hypoglossal foramen, around the mediolateral midpoint of the paroccipital process lies an ovate depression we interpret as the vagus foramen. The posteroventrally sloped portion of the paroccipital process overhangs this foramen. The locations of these foramina are consistent with those of other thalattosuchians (e.g., *Pelagosaurus* [NHMUK PV OR 32599]; *Plagiophthalmosuchus* cf. *gracilirostris* [Brusatte et al., 2016]; *Macrospondylus* [Wilberg et al., 2022]; *Teleosaurus* [Jouve, 2009]). A short distance lateral to the vagus foramen lies a laterally open notch between the paroccipital and ventrolateral processes of the otoccipital. This represents the cranioquadrate canal. As preserved, it is open laterally, though the squamosal and quadrate, which would likely have formed the lateral border if it existed, are damaged in this area. The cranioquadrate canal is fully enclosed (e.g., *Machimosaurus buffetauti* [SMNS 91415]; *Macrospondylus bollensis* [MCZ VPRA-1063]), or very nearly enclosed (e.g., *Teleosaurus cadomensis* [MNHN AC 8746; Jouve, 2009]), in all other thalattosuchians in which this region is preserved.

Basisphenoid—The basisphenoid is partially preserved, lacking its anterior region and rostrum (Figs. 2, 3). It articulates anteroventrally with the pterygoid, posteriorly with the basioccipital and dorsally with the prootic and laterosphenoid (though these latter two bones have been displaced). Only a small portion of its lateral surface is exposed, and the remainder of the description of this bone comes from the digital preparation. In ventral view, the basisphenoid is triangular in shape, with the anterior apex extending anteriorly between the quadrate processes of the pterygoid. The ventral exposure is slightly wider (mediolaterally) than long (anteroposteriorly). Posteriorly, the basisphenoid articulates with the basioccipital and forms the anterior half of the ovate opening for the median pharyngeal tube (=median Eustachian tube; Colbert, 1946). Thin lateral processes of the basisphenoid project posterolaterally, separating the quadrate from the basioccipital. The median pharyngeal foramen is rather large relative to that of other thalattosuchians, opening into a bulbous cavity within the basisphenoid which then divides laterally similar to the sphenosuchian *Almadasuchus* (Leari et al., 2020). However, these diverticula cannot be traced further with any detail.

Basioccipital—The basioccipital is nearly complete, lacking only the lateral side of the left basal tuber (Figs. 2, 3). It has not been mechanically prepared, but has been digitally prepared. The occipital condyle is ovoid, mediolaterally wider than tall. The basioccipital articulates with the otoccipital dorsolaterally and the basisphenoid anteriorly. The occipital condyle appears to be smaller than the foramen magnum (though the incomplete preservation of the foramen magnum prevents confirmation of this comparison). This is small relative to other thalattosuchians, but similar to the proportions of many sphenosuchians (e.g., *Junggarsuchus* [Ruebenstahl et al., 2022]; *Dibothrosuchus* [Wu & Chatterjee, 1993]; and *Sphenosuchus* [Walker, 1990] and protosuchids (e.g., *Protosuchus richardsoni* [UCMP 131827; Clark, 1986] and *Eopneumatosuchus colberti* [Melstrom et al., 2022]).

The occipital condyle is approximately the same size as the foramen magnum in some thalattosuchians (e.g., *Pelagosaurus typus* [NHMUK PV OR 32599] and *Teleosaurus cadomensis* [MNHN AC 8746; Jouve, 2009]). However, it is notably larger than the foramen magnum in most thalattosuchians (e.g., *Plagiophthalmosuchus* cf. *gracilirostris* [NHMUK PV OR 33095; Brusatte et al., 2016]; and *Macrospondylus bollensis* [MCZ VPRA-1063; Wilberg et al., 2022]). Ventrolateral to the occipital condyle are small, weakly developed basioccipital tubera. The tubera are mediolaterally wider than tall and are rather small relative to other thalattosuchians.

In ventral view, the basioccipital has a gently curved suture with the posterior surface of the basisphenoid. Interrupting this articulation along the midline is the median pharyngeal foramen, of which the basioccipital forms the posterior margin. Immediately posterior to the median pharyngeal foramen lies a deep fossa, interposed between the basal tubera. Poor contrast in the CT scan makes the lateral articulation between the basioccipital with the lateral wings of the basisphenoid and ventromedial portion of the otoccipital difficult to discern. However, it appears that the basioccipital forms a short portion of the medial border of the lateral Eustachian foramen, similar to *Macrospondylus bollensis* (MCZ VPRA-1063; Wilberg et al., 2022) and *Pelagosaurus typus* (NHMUK PV OR 32599).

Pterygoid—The posterior portion of the pterygoids are preserved and right and left sides appear fused (Figs. 2, 3). The preserved portion includes the posterior margin of the internal choana and part of the left pterygoid wing (flange). Posteriorly and dorsally, the pterygoid articulates with the basisphenoid. Posterolaterally, the pterygoid has a short articulation with the quadrate. As in other thalattosuchians, the pterygoid lacks a dorsal extension and contacts neither the laterosphenoid nor the trigeminal foramen. In ventral view the basisphenoid projects anteriorly like a wedge, dividing two slender, posterolateral laminae of the pterygoid. These posterolateral laminae lie between the basisphenoid medially and the pterygoid process of the quadrate laterally. At the juncture of these posterolateral laminae (at the apex of the basisphenoid ventral exposure), the posterior margin of the pterygoid possesses a relatively deep, but anteroposteriorly short concavity projecting towards the choana.

The lateral wing is short, laminar, and tapers laterally. It is inclined slightly posteroventrally. It lacks a thickened, vertically oriented flat lateral surface (torus transiliens). This structure is typically smaller in thalattosuchians than in crocodyliforms, but its total absence is surprising. This portion of the pterygoid is embedded in matrix and, while the edges of the element appear relatively clean in the digital model, it is possible that this structure is broken. Posterior to the lateral wing, the lateral margin of the pterygoid is strongly concave.

Mandible

General Comments—The posterior regions of both mandibular rami are preserved, including right (block 1; Figs. 1, 4) and left (block 3; Fig. 5) retroarticular processes. Additional smaller fragments preserve parts of the dentary and angular.

Dentary—The anterior portion of the right dentary is preserved, including part of the dentary symphysis and four alveoli containing heavily weathered teeth (Fig. 6A, B). We interpret these as the second through fifth alveoli (D2–D5). The D3 and D4 alveoli are enlarged relative to D2 and D5. They appear confluent (though it is possible that a narrow interalveolar septum is present, but not exposed) and are positioned on a slight lateral expansion of the dentary, giving it a somewhat spatulate shape and are slightly dorsal in position relative to D2 and D5. D3 and D4 are also typically the largest of the anterior dentary teeth in most other thalattosuchians, also with alveoli that are

confluent or have a very narrow interalveolar space (e.g., *Pelagosaurus typus* [BRLSI M1413; Pierce and Benton, 2006]; *Macrospondylus bollensis* [NHMUK PV R 12011]; *Proexochokefalos heberti* [MNHN 1890-13]; *Lemmingsuchus obtusidens* [NHMUK PV R 3168; Johnson et al., 2017]; *Thalattosuchus superciliosus* [NHMUK PV OR 46323]). The symphyseal surface preserves a series of grooves radiating anteriorly and posteriorly from the Meckelian fossa, located medial to the D5 alveolus and extending posteriorly to the broken posterior end of the specimen. This would have formed a typical Class III mandibular symphysis (sensu Scapino, 1981), shared by other thalattosuchians and most crocodyliforms (Holliday & Nesbitt, 2013).

A second small fragment of the left dentary is preserved (Fig. 6C, D). This portion comes from the posterior region of the dentary, potentially posterior to the symphysis. Its lateral surface is ornamented with deep grooves ventrally, which become less distinct dorsally. Four teeth are preserved, though mediolaterally crushed. Just medial to the toothrow, the medial shelf of the dentary possesses an elongate groove, paralleling the toothrow. This groove was likely for articulation of the anterior process of the coronoid, which in thalattosuchians is highly elongate and abuts the posterior portion of the toothrow. An anteriorly elongate coronoid is also present in most sphenosuchians (Ruebenstahl et al., 2022), though in these taxa the anterior process extends along most of the dentary toothrow. Medially this fragment of the dentary would have articulated with the splenial, but no trace of this element is preserved.

A third mandibular fragment potentially preserves the posterolateral surface of the left dentary articulating with a small fragment of the angular (Fig. 6E). The lateral surface of this dentary fragment is ornamented by fine anteroposteriorly directed striations and bears an elongate groove spanning its preserved length. This groove lies dorsal to the dentary-angular articulation and is not quite parallel with this suture, diverging anteriorly. This groove is likely a small portion of the surangulodentary groove (sensu Young et al., 2012) common among thalattosuchians, though it is not as deeply excavated as in metriorhynchids.

Surangular—The posterior portions of both right and left surangulars are preserved (Figs. 4, 5). On the right side, the posterior-most portion of the surangular is preserved on the lateral surface of the retroarticular process. The preserved portion has a horizontal suture with the angular ventrally and articulates with the articular medially. Its surface is marked with distinct pits anteriorly that become less distinct posteriorly, such that the posterior-most portion is smooth. It nearly reaches the posterior end of the retroarticular process. The left surangular is exposed in medial view, anterior to the glenoid fossa. It is gently concave, articulating with the angular ventrally. Near the anterior end of the preserved portion lies a circular foramen on the medial surface, located near the dorsoventral midpoint of this surface. A similar foramen is present in *Pelagosaurus* (NHMUK PV OR 32599), but that of *T. hingleyae* is more anteriorly positioned.

Angular—The posterior portion of each angular is preserved (Figs. 4, 5), as well as a small, more anterior fragment of the left angular articulating with the dentary described above (Fig. 6E). The lateral surface of the small fragment articulating with the dentary is ornamented with strong, anteroposteriorly aligned grooves. The preserved posterior parts of the angular are ornamented with distinct pits. These pits begin to dissipate posteriorly, beginning at the level of the glenoid fossa, becoming smooth approximately half way along the length of the retroarticular process. The angular articulates with the dentary anteriorly, the articular and prearticular medially, and the surangular dorsally. The ventral edge of the articular forms a medially curved

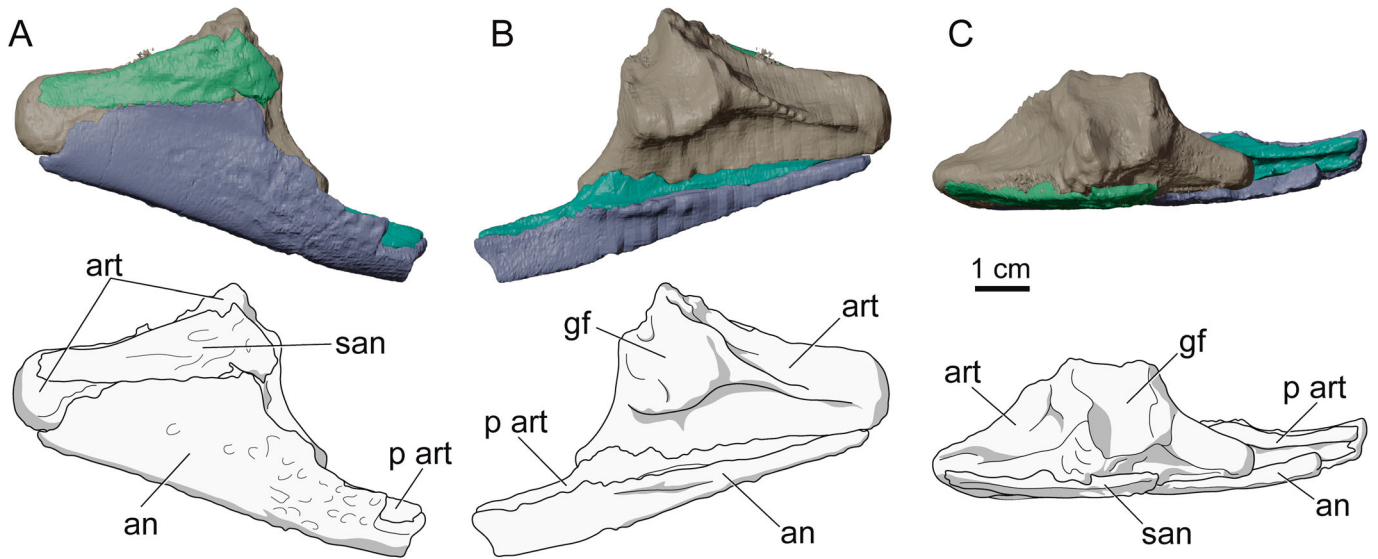


FIGURE 4. Right retroarticular process of *Turnersuchus hingleyae* gen. et sp. nov. (LYMPH 2021/45). **A**, digital model and line interpretation in lateral view; **B**, digital model and line interpretation in medial view; **C**, digital model and line interpretation in dorsal view. **Abbreviations:** an, angular; art, articular; gf, glenoid fossa; p art, prearticular; san, surangular.

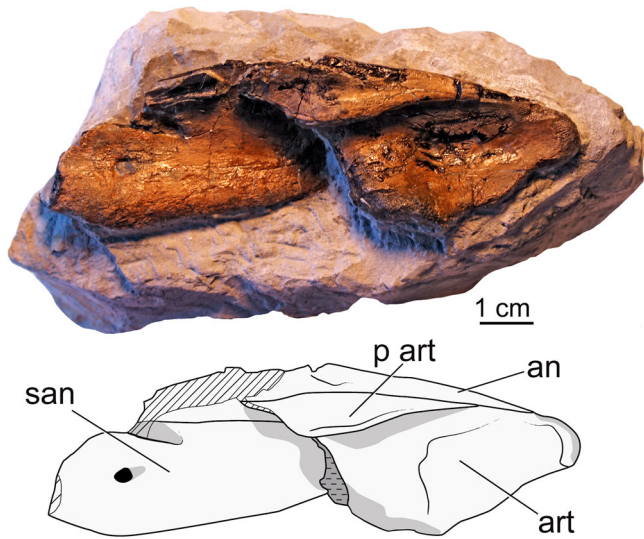


FIGURE 5. Photograph and line interpretation of the posterior region of left mandibular ramus of *Turnersuchus hingleyae* gen. et sp. nov. (LYMPH 2021/45) exposed in ventral view. **Abbreviations:** an, angular; art, articular; p art, prearticular; san, surangular.

shelf, in which the prearticular and articular sit. Posteriorly it extends nearly to the tip of the retroarticular process.

Prearticular—A prearticular bone is present as in other thalattosuchians (Figs. 4, 5). It is an elongate triangular bone articulating with the articular dorsally and the angular laterally and ventrally. Posteriorly it extends approximately two thirds the length of the retroarticular process. Its anterior extent is unknown as it is damaged on both sides.

Articular—Both right and left articulars are nearly complete. The left is exposed in ventral view (Fig. 5), while the right is partially visible in lateral view (Fig. 1). The right articular has been digitally segmented so all portions can be described (Fig. 4). The

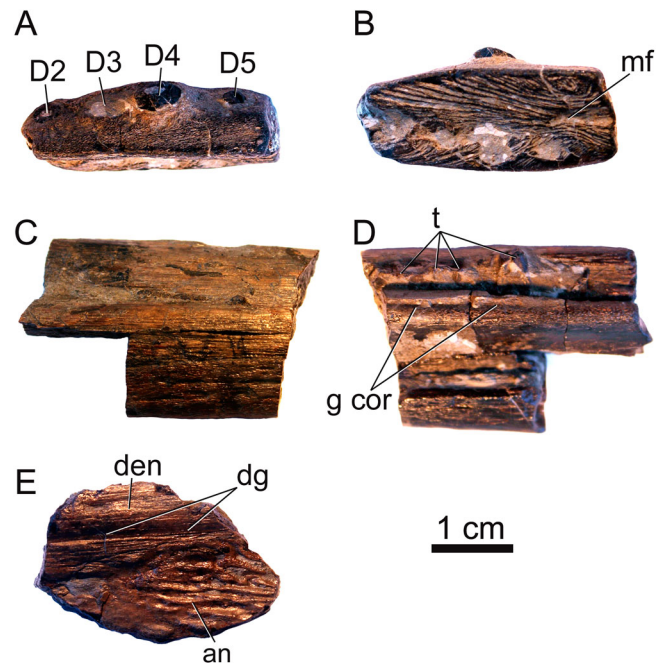


FIGURE 6. Mandibular fragments of *Turnersuchus hingleyae* gen. et sp. nov. (LYMPH 2021/45). **A**, right anterior dentary fragment in dorsal view; **B**, medial view of the same; **C**, posterior left dentary fragment in lateral view; **D** medial view of the same; **E**, posterior left mandibular fragment in lateral view. **Abbreviations:** an, angular; D1–D5, second through fifth dentary alveoli and/or teeth; den, dentary; dg, dentary groove, g cor, groove for articulation of anterior process of coronoid; mf, Meckelian fossa; t, posterior dentary teeth.

articular articulates with the surangular and angular laterally, and the prearticular ventrally. The articular forms the rectangular glenoid fossa and the triangular retroarticular process. The medial surface of the articular is concave, with the medial shelf of the retroarticular process and medial half of the glenoid

fossa overhanging its surface. The glenoid fossa consists of medial and lateral concavities separated by a subtle ridge. The medial portion of the fossa extends slightly further ventrally, to articulate with the dorsoventrally deeper medial hemicondyle of the quadrate. The glenoid fossa is bordered anteriorly by a low, straight, transversely oriented ridge and posteriorly by a strong sigmoid ridge. Laterally, the glenoid may have been bordered by the surangular. This region is damaged, but it does not appear that the surangular would have contributed to the articular surface.

The retroarticular process is triangular in dorsal view with its length slightly exceeding the width of the glenoid fossa. The retroarticular process of *Turnersuchus* is considerably shorter than that of most teleosauroids (e.g., *Plagiophthalmosuchus gracilirostris* [NHMUK PV OR 15500]; *Mycterosuchus nasatus* [NHMUK PV R 2617; Andrews, 1913]; *Macrospodylus bollensis* [MCZ VPRA-1063; Wilberg et al., 2022]; *Indosinosuchus potamosiamensis* [PRC-11; Martin et al., 2019]), and more closely resembles the morphology of basally branching metriorhynchoids (e.g., *Pelagosaurus* [BRLSI M1413; Pierce and Benton, 2006]; *Teleidosaurus calvadosii* [NHMUK PV R 2681]; *Zoneait nargorum* [UOMNH F39539; Wilberg, 2015a]). The dorsal surface of the retroarticular process houses a broad fossa for the attachment of *M. depressor mandibulae*. In most thalattosuchians, a long crest divides the dorsal surface into medial and lateral fossae (e.g., *Pelagosaurus* [BRLSI M1413; Pierce & Benton, 2006]; *Teleidosaurus calvadosii* [NHMUK PV R 2681]; *Macrospodylus bollensis* [MCZ VPRA-1063; Wilberg et al., 2022]). In *Turnersuchus*, a faint crest begins along the posterior margin of the glenoid, but flattens out about one third the length of the fossa. The posterior end of the articular is ovate and convex, slightly exceeding the posterior end of the surangular and angular.

Axial Skeleton

General Comments—The vertebral column of *Turnersuchus hingleyae* is not completely preserved. Block 1, which was CT-scanned, includes the last five cervical and the first five dorsal vertebrae which are preserved in articulation, plus one isolated cervical vertebra. Additionally, four articulated dorsal vertebrae are preserved in block 2, which represent more posterior vertebrae and are not continuous with the series preserved in block 1. Sacral vertebrae are not preserved and only eight caudal vertebrae are present, preserved as four isolated pairs of vertebrae, two of which are preserved in blocks 4 and 5. In total, 23 vertebrae are preserved: six cervical vertebrae, nine dorsal vertebrae, and eight caudal vertebrae. CT data were obtained for all cervical vertebrae and five of the dorsal vertebrae. All vertebrae of *T. hingleyae* are amphicoelous, as is typical for most non-eusuchian crocodylomorphs.

Cervical Vertebrae and Ribs—The last five cervical vertebrae are preserved in articulation in block 1, with their right side exposed (Fig. 1). Additionally, there is an isolated cervical vertebra in the same block, which was probably originally located anterior to these five articulated vertebrae (i.e., between the atlas-axis and the last five cervical vertebrae) and has the dorsal surface of its centrum exposed. The cylindrical centra are slightly anteroposteriorly longer than dorsoventrally high. The anterior and posterior articular surfaces are slightly concave. In more anterior vertebrae, these articular surfaces are slightly higher than wide, whereas in more posterior ones the centra are nearly as high as wide, forming a more circular surface (Fig. 7A–E). In ventral view, cervical centra are roughly hourglass-shaped, due to the thick margins of the anterior and posterior articular surfaces of the centra (Fig. 7E). As in all thalattosuchians, cervical or dorsal vertebrae do not bear distinctive hypapophyses. The ventral surface of the cervical

centra of *Turnersuchus hingleyae* exhibits a ventral keel ranging anteroposteriorly through the midline the vertebrae (Fig. 7E), similar to the condition seen in other thalattosuchians, such as *Indosinosuchus potamosiamensis* (PRC-18; Martin et al. 2019), *Enaliosuchus macrospodylus* (MB.R.1943.3; Sachs et al. 2020) and *Pelagosaurus typus* (BSGP 1890 I 510/1).

The cervical transverse processes, or diapophyses, and parapophyses of *Turnersuchus hingleyae* bear the facets for the attachment of the cervical ribs (tuberculum and capitulum). The parapophyses are located anteroventrally on the centrum, and project ventrolaterally (Fig. 7A, B). The diapophyses project from around anteroposterior midpoint of each vertebra, originating on the lateral surface of the neural arch base, and from slightly more dorsally in the last cervical vertebra (a pattern also observed in other thalattosuchians, including teleosauroids and metriorhynchoids; Wilkinson et al., 2008). The diapophyses are strongly inclined ventrolaterally, although slightly less so in the final cervical vertebra (Fig. 7A, B). All five articulated cervical vertebrae preserve the neural arches. Additionally, the isolated cervical vertebra also preserves part of its left neural arch.

The prezygapophyses and postzygapophyses of the cervical vertebrae are at the same height, dorsal to the neural arches (Fig. 7A–E). Prezygapophyses are anterodorsally oriented in lateral view (Fig. 7C) and the articular facets face dorsomedially at an angle of nearly 45°, as in other thalattosuchians, such as *Pelagosaurus typus* (BRLSI M3578; Pierce & Benton, 2006), *Enaliosuchus macrospodylus* (MB.R.1943.6; Sachs et al., 2020), and *Charitomenosuchus leedsi* (NHMUK PV R 3806; Andrews, 1913). The prezygapophyses of more posterior cervical vertebrae do not differ much, in shape or orientation, from the anterior ones. Postzygapophyses are slightly larger than prezygapophyses, but also do not differ much from more anterior to more posterior cervical vertebrae. Postzygapophyses exhibit suprapostzygapophyseal laminae (sensu Pol, 2005) on their dorsal surfaces, as in other crocodylomorphs, such as the notosuchians *Notosuchus terrestris* (MACN-RN 1037; Pol, 2005) and *Araripesuchus tsangatsangana* (FMNH PR 2297; Turner, 2006), but also observed in thalattosuchians, such as in *Torvoneustes carpenteri* (BRSMG Cd7203; Wilkinson et al., 2008) and *Teleidosaurus calvadosii* (MPV 20120.3.45; Hua, 2020). Both suprapostzygapophyseal laminae join each other medially, forming the neural spine dorsally. All five articulated cervical vertebrae have their neural spine completely preserved, although in the last three vertebrae the dorsal-most tips of the neural spine are displaced from their original position (Fig. 7A–E). All five neural spines are rounded dorsally and are slightly shorter dorsoventrally than the dorsoventral height of the centrum. Neural spines of more posterior cervical vertebrae appear to be proportionally longer anteroposteriorly than more anterior ones, although they are broken dorsally, preventing accurate assessment.

The five articulated cervical vertebrae also preserve their right cervical ribs (Fig. 7A–E). The ribs are not attached to the vertebrae, but are preserved only slightly displaced from their original positions. The ribs are “double-headed” and exhibit a typical crocodylomorph morphology of postaxial cervical ribs (Mook, 1921). The first four ribs of the series are very similar in shape to each other, with a mediolaterally flattened shaft extending parallel to the longitudinal axis of the vertebral column, and a pair of processes, tuberculum and capitulum, that attach to the diapophysis and parapophysis, respectively. The shaft of these four ribs bears anterior and posterior processes, with the posterior being more elongated. In these ribs, the tuberculum and capitulum project distally from their attachment with diapophysis and parapophysis, making them perpendicular to the shaft of the ribs. The tuberculum is slightly longer than the capitulum, whereas the capitulum is more anteriorly positioned, so that the two processes are not exactly in parallel. The first three ribs of the series

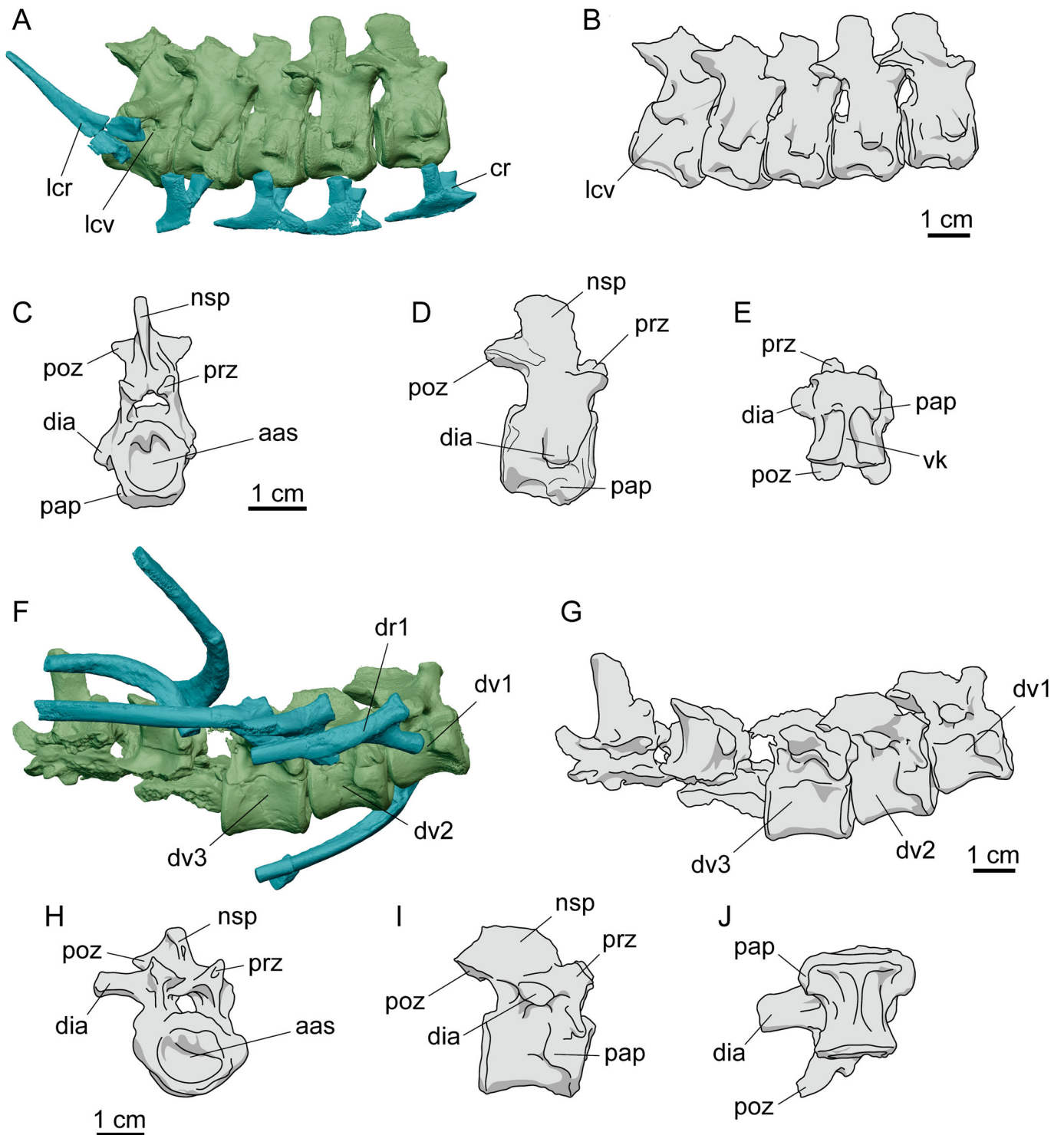


FIGURE 7. Cervical and dorsal vertebrae of *Turnersuchus hingleyae* gen. et sp. nov. (LYMPH 2021/45). **A**, digital model of vertebral series of the last five cervical vertebrae with cervical ribs in right lateral view; **B**, line interpretation of same (without the ribs); **C**, line interpretation of the first cervical vertebra of the series in anterior view; **D**, line interpretation of same in right lateral view; **E**, line interpretation of same in ventral view; **F**, digital model of vertebral series of the first five dorsal vertebrae with ribs in right lateral view; **G**, line interpretation of same (without the ribs); **H**, line interpretation of the second dorsal vertebra of the series in anterior view; **I**, line interpretation of same in right lateral view; **J**, line interpretation of same in ventral view. **Abbreviations:** **aas**, anterior articular surface; **cr**, cervical rib; **dr1**, first dorsal rib; **dv1**, first dorsal vertebra; **dv2**, second dorsal vertebra; **dv3**, third dorsal vertebra; **dia**, diapophysis; **lcr**, last cervical rib; **lcv**, last cervical vertebra; **nsp**, neural spine; **pap**, parapophysis; **poz**, postzygapophysis; **prz**, prezygapophysis; **vk**, ventral keel.

are nearly completely preserved, whereas the fourth lacks the anterior- and posterior-most processes of the shaft. The last cervical rib is comparatively more elongated than the other four, although not as long as the dorsal ribs. In this last cervical rib, tuberculum and capitulum are not perpendicular to the shaft, but rather look like direct extensions of the shaft, projecting posteriorly from the diapophysis and parapophysis.

Dorsal Vertebrae and Ribs—The first five dorsal vertebrae are preserved in articulation in block 1, with their right and ventral surfaces mostly exposed (Fig. 1). There are also four dorsal vertebrae preserved in articulation in block 2 (Fig. 8), the exact position of which in the vertebral column cannot be verified, but were probably only slightly posterior to the vertebral series preserved in block 1. We will focus our description of the dorsal vertebrae on the ones preserved in block 1 (Fig. 7F–J), given that these were CT-scanned, but the vertebrae in block 2 will be mentioned when appropriate.

Only the first three vertebrae of the series in block 1 preserve their centra, which are missing in the last two vertebrae of the series. Similar to the cervical vertebrae, the cylindrical centra of dorsal vertebrae of *Turnersuchus hingleyae* are anteroposteriorly longer than dorsoventrally high, with more posterior vertebrae becoming even longer anteroposteriorly (a pattern confirmed in the vertebrae preserved in block 2), as also seen in *Indosinosuchus potamosiamensis* (PRC-20 and PRC-21; Martin et al. 2019), *Enaliosuchus macrospondylus* (MB.R.1943.6; Sachs et al. 2020), *Charitomenosuchus leedsi* (NHMUK PV R 3806;

Andrews, 1913) and *Cricosaurus araucanensis* (MLP 72-IV-7-1; Herrera et al. 2013). The concave anterior and posterior articular surfaces of the centra are similar to the ones observed in the posteriormost cervical vertebrae, with roughly circular surfaces, nearly as high as wide (Fig. 7H). The centra exhibit an hourglass shape in ventral view, as a consequence of the thicker margins of the anterior and posterior articular surfaces, similar to the cervical centra (Fig. 7J). However, in the first two dorsal vertebrae, the parapophyses project from a level ventral to the neural arches and are located near the anterior articular surface, which gives these two vertebrae laterally expanded anterior halves of the centra in ventral view. The dorsal vertebrae of *T. hingleyae* lack the clear ventral keel seen in cervical centra, a condition also observed in *Magyarosuchus fitosi* (MTM V.97.26; Ósi et al., 2018), *Indosinosuchus potamosiamensis* (RMH uncatelaged; Martin et al. 2019) and *Enaliosuchus macrospondylus* (Sachs et al. 2020).

The parapophyses of the first two dorsal vertebrae of *Turnersuchus hingleyae* are more ventrally located (i.e., placed on the centra) than those of more posterior vertebrae, in which the parapophyses project laterally from the same level of the neural arches, more closely located to the transverse processes (Fig. 7G, H). The transverse processes of the first two vertebrae are nearly cylindrical and project laterally from the neural arches, whereas those of the remaining dorsal vertebrae become increasingly more inclined dorsally and anterodorsally flat. Similar to the cervical vertebrae, the parapophyses of dorsal vertebrae



FIGURE 8. Block 2 containing four dorsal vertebrae, the right ulna, and dorsal ribs and gastralia of *Turnersuchus hingleyae* gen. et sp. nov. (LYMPH 2021/45).

are located near the anterior margin of the centra in lateral view, whereas the transverse processes are placed near the middle of the anteroposterior extension of the centra. This is similar to the condition of *Enaliosuchus macrospondylus* (Sachs et al., 2020) and *Magyarosuchus fitosi* (MTM V.97.26.; Ősi et al., 2018), but different from what is seen in *Charitomenosuchus leedsi* (NHMUK PV R 3806; Andrews, 1913), in which the parapophyses are not as anteriorly located, particularly in more anterior dorsal vertebrae.

The neural arches are present in the first three vertebrae of the series and also partially preserved in the two remaining vertebrae. Nevertheless, the preservation of the region of the neural arches is not ideal, particularly in more posterior vertebrae, preventing a clear assessment of the morphology of the neural spines. In more anterior dorsal vertebrae, the prezygapophyses and postzygapophyses are better preserved and located dorsal to the neural arches in lateral view (Fig. 7G, I). In comparison to the prezygapophyses of cervical vertebrae, those of dorsal vertebrae have their articular facets more inclined and slightly more turned medially.

The first three dorsal vertebrae in block 1 preserve the proximal portions of their associated ribs nearly in articulation, whereas three other partial dorsal ribs are also preserved in the block but not in articulation. Some dorsal vertebrae and gastralia are also preserved in block 2 (Fig. 8). The first three dorsal ribs of *Turnersuchus hingleyae* exhibit a proximal morphology similar to that of other crocodylomorphs (Mook, 1921), with the capitulum longer than the tuberculum. The tuberculum is parallel with the axis of the rib shaft, whereas the capitulum forms an angle of nearly 45° with the shaft. The third rib is better preserved, exhibiting a long and slightly curved shaft that projects posteriorly at least to the level of the fifth dorsal vertebra.

Caudal Vertebrae—Two pairs of caudal vertebral centra are partially preserved in blocks 4 and 5 (Fig. 9A, B). Additionally, two other pairs of vertebral centra are present (Fig. 9C, D), which are probably caudal vertebrae, but the poor preservation prevents an unambiguous assignment. Therefore, we focus our description of caudal vertebrae on the pairs preserved in blocks 4 and 5. After the submission of this work, an additional pair of partial vertebral centra associated with the holotype was donated to LYMPH and repositioned under the same specimen number (LYMPH 2021/45). These elements provide no additional information beyond that of the other elements. Photographs of this material are available at www.morphobank.org/permalink/?P4271.

Using *Magyarosuchus fitosi* (MTMV.97.28.; Ősi et al., 2018) and *Cricosaurus araucanensis* (MLP 73-II-27-6; Herrera et al., 2013) as reference specimens (given the fairly complete description of their caudal series), the caudal vertebrae in these two blocks probably represent anterior (block 4) and posterior (block 5) caudal vertebrae. The anterior and posterior articular surfaces are concave and the ventral surface does not bear any ridge. As in other vertebrae of *Turnersuchus hingleyae*, the centra are anteroposteriorly longer than dorsoventrally high. The centra in block 5 exhibit the typical morphology of more posterior caudal vertebrae, with mediolaterally compressed lateral surfaces and strongly concave ventral surfaces, which gives the centra a more rectangular look in lateral view, similar to what is seen in *Neosteneosaurus edwardsi* (NHMUK PV R 3701; Andrews, 1913).

Appendicular Skeleton

Pectoral Girdle—The right coracoid and scapula are preserved in articulation in block 1, with their lateral surfaces exposed (Fig. 10). The coracoid preserves only its proximal end, lacking the shaft and distal portion, whereas the scapula is almost completely preserved, but broken. The bones are larger and longer than

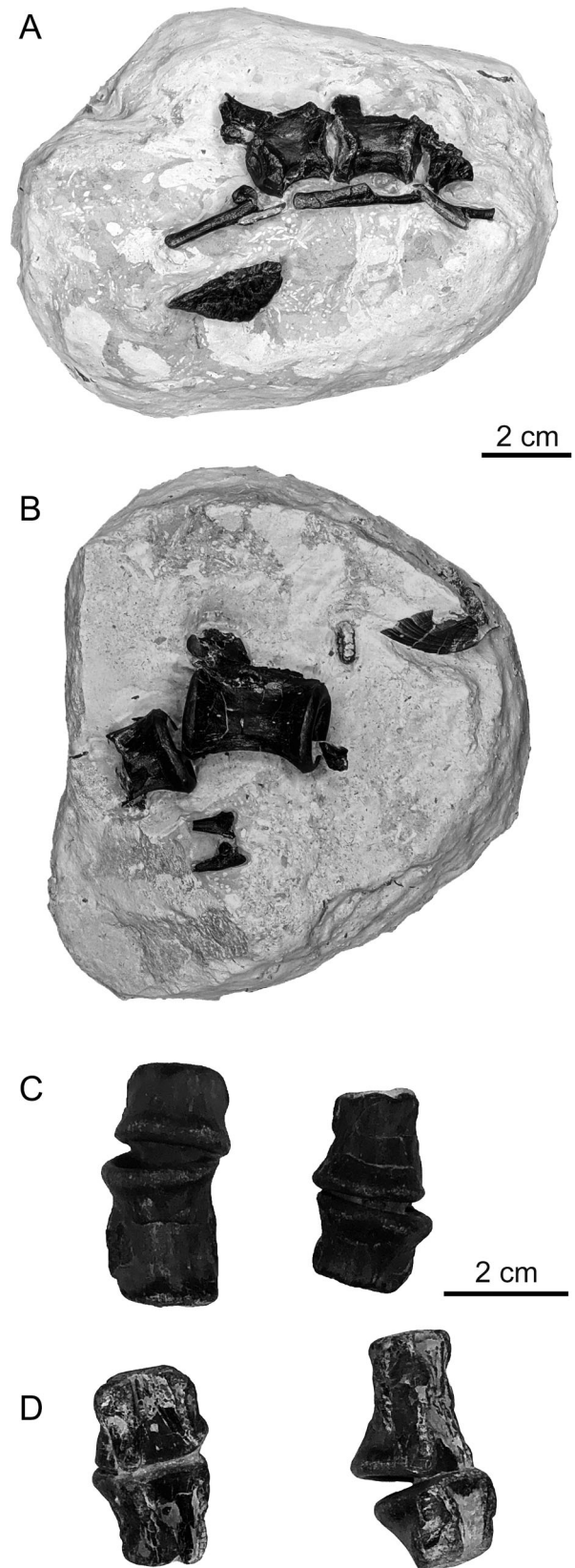


FIGURE 9. Caudal vertebrae of *Turnersuchus hingleyae* gen. et sp. nov. (LYMPH 2021/45). **A**, block 5 containing caudal vertebrae from a relatively posterior position in series; **B**, block 4 containing one complete and one partial caudal vertebra from a relatively anterior position in the series; **C**, pair of likely caudal centra; **D**, second pair of likely caudal centra.

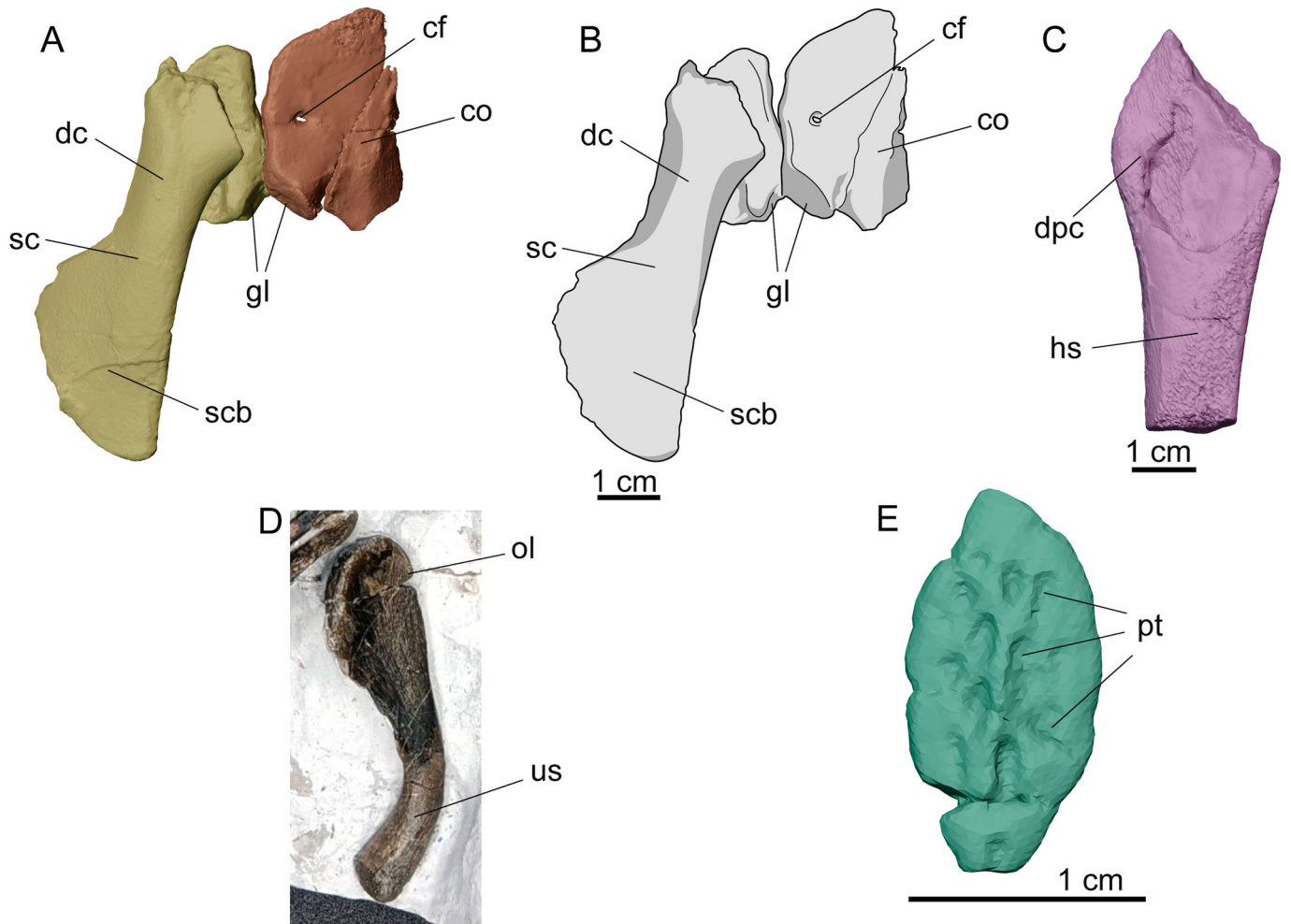


FIGURE 10. Appendicular bones of *Turnersuchus hingleyae* gen. et sp. nov. (LYMPH 2021/45). **A**, digital model of the right scapula and coracoid in lateral view; **B**, line interpretation of same; **C**, digital model of the proximal right humerus in medial view; **D**, right ulna in medial view; **E**, digital model of dorsal (caudal?) osteoderm in dorsal view. **Abbreviations:** co, coracoid; cf, coracoid foramen; dc, deltoid crest; dpc, deltopectoral crest; gl, glenoid fossa; hs, humeral shaft; ol, olecranon process; pt, pits; sc, scapula; scb, scapular blade; us, ulnar shaft.

those of some metriorhynchids, such as *Cricosaurus araucanensis* (MLP 72-IV-7-1; Herrera et al. 2013), in which the pectoral girdle and forelimb bones are extremely reduced in size. The proximal portion of the coracoid is similar to that of *Magyarosuchus fitosi* (MTM V.97.7.; Ósi et al., 2018) and *Charitomenosuchus leedsi* (NHMUK PV R 3806; Andrews, 1913), with its lateral surface bearing an oval-shaped coracoid foramen and its posterodorsal corner bearing a nearly flat surface that contributes to the glenoid fossa. The scapula of *Turnersuchus hingleyae* is relatively flat, with expanded and nearly equally wide distal and proximal ends (scapular blade and scapulocoracoid articulation, respectively), which gives it an almost bow-tie shape, similar to the scapulae of *Pelagosaurus typus* (BRLSI M3578; Pierce & Benton, 2006) and *Macrospondylus bollensis* (SMNS 51563; Mueller-Töwe, 2006), but slightly different from the more rod-like shape of the scapula of *Charitomenosuchus leedsi* (NHMUK PV R 3806; Andrews, 1913). The anterior margin of the scapula of *Turnersuchus* is more strongly concave than is the posterior margin. This differs from the more symmetrical scapula of *Pelagosaurus* (BRLSI M1418; Pierce & Benton, 2006), but is shared with some teleosauroids (e.g., *Indosinosuchus potamosiamensis* [Martin et al., 2019]; *Lemmysuchus obtusidens* [Johnson et al., 2017]). The proximal most portion of the scapula is

detached from the remainder of the bone, making the proximal end slightly displaced from the scapular shaft. Nevertheless, some features of the proximal end can still be observed, such as the faint deltoid crest. Both scapula and coracoid make a broad contact and contribute nearly equally in the glenoid fossa.

Forelimb—The proximal end of the right humerus is preserved in block 1, with its medial surface exposed and not in articulation with the pectoral girdle bones (indeed, the articulation surface is not preserved; Figs. 1, 10). The humerus of *Turnersuchus hingleyae* is relatively flat and broad, with the preserved portion of the shaft nearly straight. The region is not ideally preserved, but the deltopectoral crest seems relatively small, similar to that of *Zoneait nargorum* (UOMNH F39539; Wilberg, 2015a) or *Pelagosaurus* (UH 4; Mueller-Töwe, 2006) which show a dorsoventrally thin and reduced crest, with probably less than one-third of the humerus length, but not as reduced as the crests of metriorhynchids (e.g., *Cricosaurus araucanensis*; Herrera et al., 2013). The right ulna is preserved in block 2, lacking only its distal end and with its medial surface exposed (Fig. 8). The proximal surface is twice as wide as the ulnar shaft. The ulna is not as strongly “J”-shaped as those of *Zoneait nargorum* (UOMNH F39539; Wilberg, 2015a) and *Neosteneosaurus edwardsi* (NHMUK PV R 3701; Andrews, 1913), due to a less developed

olecranon process. Instead, the ulnar shaft of *T. hingleyae* is more curved than in these two taxa. Similar to *Zoneait nargorum* (UOMNH F39539; Wilberg, 2015a) and *Neosteneosaurus edwardsi* (NHMUK PV R 3701; Andrews, 1913), the ulna of *T. hingleyae* is reduced in size relative to the humerus (less than half of the humeral length), but proportionally larger than those of metriorhynchids (e.g., *Cricosaurus araucanensis*; MLP 72-IV-7-1; Herrera et al., 2013).

Osteoderms

Only one dorsal osteoderm is preserved, in block 1 (Figs. 1, 10). It is oval-shaped, with a faint anteroposterior dorsal keel. Its shape and relatively small size suggest that it corresponds to a distal caudal osteoderm. Very few distal caudal osteoderms are reported for thalattosuchians, but the osteoderm of *Turnersuchus hingleyae* resembles one of the caudal osteoderms assigned to *Charitomenosuchus leedsii* (NHMUK PV R 3806; Andrews, 1913). It has a pitted ornamentation on its dorsal surface, with the pits being well separated from one another.

RESULTS

Phylogenetic Analyses

Analysis of the Wilberg et al. (2019) matrix resulted in eight most parsimonious trees (MPTs) with a length of 1774 steps, a consistency index (CI) of 0.309 and a retention index (RI) of 0.753 (Fig. 11A). The new taxon is recovered as the earliest diverging thalattosuchian, with the remainder of Thalattosuchia consisting of a monophyletic Teleosauroidea and Metriorhynchoidea. Four unambiguous synapomorphies unite *T. hingleyae* with Thalattosuchia: (1) presence of a posterolaterally directed fossa on posterolateral margin of squamosal (82.1); (2) insignificant/weakly developed squamosal overhang of lateral temporal region (84.0); (3) triangular retroarticular process posterodorsally curving and elongate (300.3); and (4) glenoid surface of coracoid extended on an oblique plane and glenoid lip facing outwards and posteroventrally (365.2).

Analysis of the matrix of Herrera et al. (2021) results in 165,888 MPTs with a length of 1783 steps, a CI of 0.403, and a retention index of 0.834 (Fig. 11B). This analysis also recovers *T. hingleyae* as the earliest diverging thalattosuchian (with *Eopneumatosuchus* as sister to this clade). Five characters unite *T. hingleyae* with Thalattosuchia: (1) complex dorsal surface of skull roof (110.0); (2) longitudinal groove absent from dorsolateral edge of squamosal (154.0); (3) prootic exposed in dorsal view (245.0); (4) quadrate lacking contact with laterosphenoid (264.0); and (5) anteroventral (orbital) process of quadrate free of bony attachment along anteromedial surface but contacts pterygoid ventrally (266.2).

While numerous synapomorphies support *Turnersuchus* as a member of Thalattosuchia in each dataset, only a single character in each unambiguously supports the exclusion of *Turnersuchus* from Metriorhynchoidea + Teleosauroidea. For the Wilberg et al. (2019) dataset, this character is the lack of pendulous basioccipital tubera (217.1). For the Herrera et al. (2021) dataset, the character is the presence of a more strongly concave anterior than posterior margin of the scapula (426.1). For the Wilberg et al. (2019) matrix in trees one step longer than the most parsimonious, *Turnersuchus* is alternatively recovered as the earliest-branching metriorhynchoid, the earliest-branching teleosauroid, or sister to *Plagiophthalmosuchus* at the base of Teleosauroidea. Trees one step longer than the most parsimonious for the Herrera et al. (2021) matrix include *Turnersuchus* as the basal-most metriorhynchoid, basal-most teleosauroid, or *Plagiophthalmosuchus* (and the highly fragmentary

Peipehsuchus) shifting to the stem of Thalattosuchia (sometimes in a more basal position than *Turnersuchus*).

Time-calibration of the Topologies

Results of the Bayesian tip-dating analyses are presented in Figure 12 (time-scaled tree files are available on MorphoBank; www.morphobank.org/permalink/?P4271). Analysis of the Wilberg et al. topology recovers the origination time for Thalattosuchia constrained between 221.2 and 195.09 Ma (95% highest posterior density, HPD), spanning from the Norian to the Hettangian, with a median age of 209.01 Ma, within the Norian. Analysis of the Herrera et al. topology recovers a Sinemurian (195.44 Ma) median origination age for Thalattosuchia, with the 95% HPD ranging from the Norian to Pliensbachian (204.43–190.12 Ma).

DISCUSSION

Plesiomorphic Thalattosuchian Condition

Turnersuchus is here recovered as the earliest diverging thalattosuchian (sister to Metriorhynchoidea + Teleosauroidea; Fig. 11A, B). In many aspects it resembles *Plagiophthalmosuchus* and *Pelagosaurus*, the earliest diverging members of Teleosauroidea and Metriorhynchoidea, respectively. *Turnersuchus* shares a number of features with *Plagiophthalmosuchus* and *Pelagosaurus*, helping to cement these as plesiomorphic traits for the group. These include: large supratemporal fenestrae; lack of a flat skull table; ornamentation of the bones of the lateral temporal bar; presence of a squamosal facet; quadrate forming anterior, dorsal, and ventral margins of the external otic aperture (squamosal excluded from aperture margin); fused pterygoids (at least posteriorly); broad ventrolateral process of the otoccipital overlapping the dorsal surface of quadrate; and broad exposure of prootic on lateral braincase wall. However, it differs from both in two key ways that one might expect from an earlier diverging member of the group: (1) the quadrate is less integrated with the braincase than other thalattosuchians (in *Turnersuchus*, the orbital process of quadrate is broadly separated from the trigeminal foramen and laterosphenoid); (2) it possesses more poorly developed basioccipital tubera.

A major evolutionary trend in crocodylomorphs is the development of a robust, akinetic skull (Walker, 1972, 1990; Benton & Clark, 1988; Busbey, 1995; Clark et al., 2004; Pol et al., 2013). One of the primary drivers of this trend involves the expansion of the quadrate such that it articulates extensively with bones of the braincase. In early crocodylomorphs such as *Sphenosuchus*, the head of the quadrate shifts anteriorly and medially, developing a contact with the prootic (Walker, 1990). Further articulation of the quadrate with the braincase developed in the later-diverging sphenosuchians. In *Junggarsuchus*, the quadrate develops a tight articulation with the posterior skull via sutures with the otoccipital (Clark et al., 2004; Pol et al., 2013). The quadrate becomes further articulated with the braincase in *Almadasuchus*, with extensive sutures between the quadrate, otoccipital, and basisphenoid. Among crocodyliforms, this trend continues with the anteromedial expansion of the quadrate, expanding over the prootic to contact the laterosphenoid along the lateral wall of the braincase (Benton & Clark, 1988; Pol et al., 2013; Melstrom et al., 2022) and the parietal in the supratemporal fossa (Leardi et al., 2020).

In terms of quadrate morphology, thalattosuchians appear intermediate between late-diverging sphenosuchians, and crocodyliforms. The thalattosuchian quadrate is tightly sutured with the otoccipital and basisphenoid. However, it lacks the broad expansion onto the lateral braincase wall typical of crocodyliforms. The medial part of the primary head of the thalattosuchian

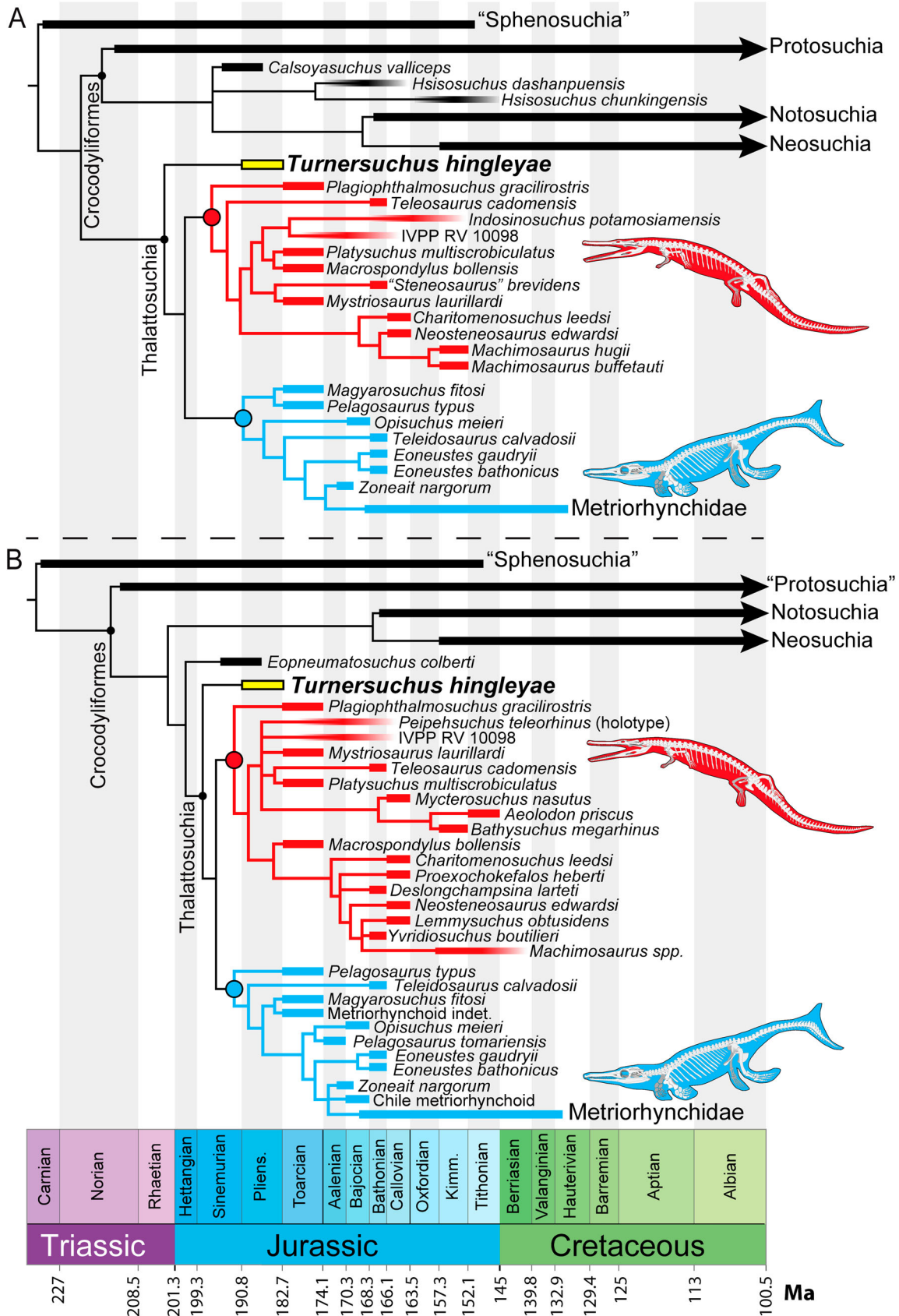


FIGURE 11. Phylogenetic placement of *Turnersuchus hingleyae* gen. et sp. nov. (in bold) with trees calibrated to stratigraphy. **A**, strict consensus of eight most parsimonious trees of 1774 steps (CI = 0.309; RI = 0.753) resulting from analysis based on the dataset of Wilberg et al. (2019); **B**, strict consensus of 165,888 most parsimonious trees of 1783 steps (CI = 0.403; RI = 0.834) resulting from analysis based on the dataset of Herrera et al. (2021).

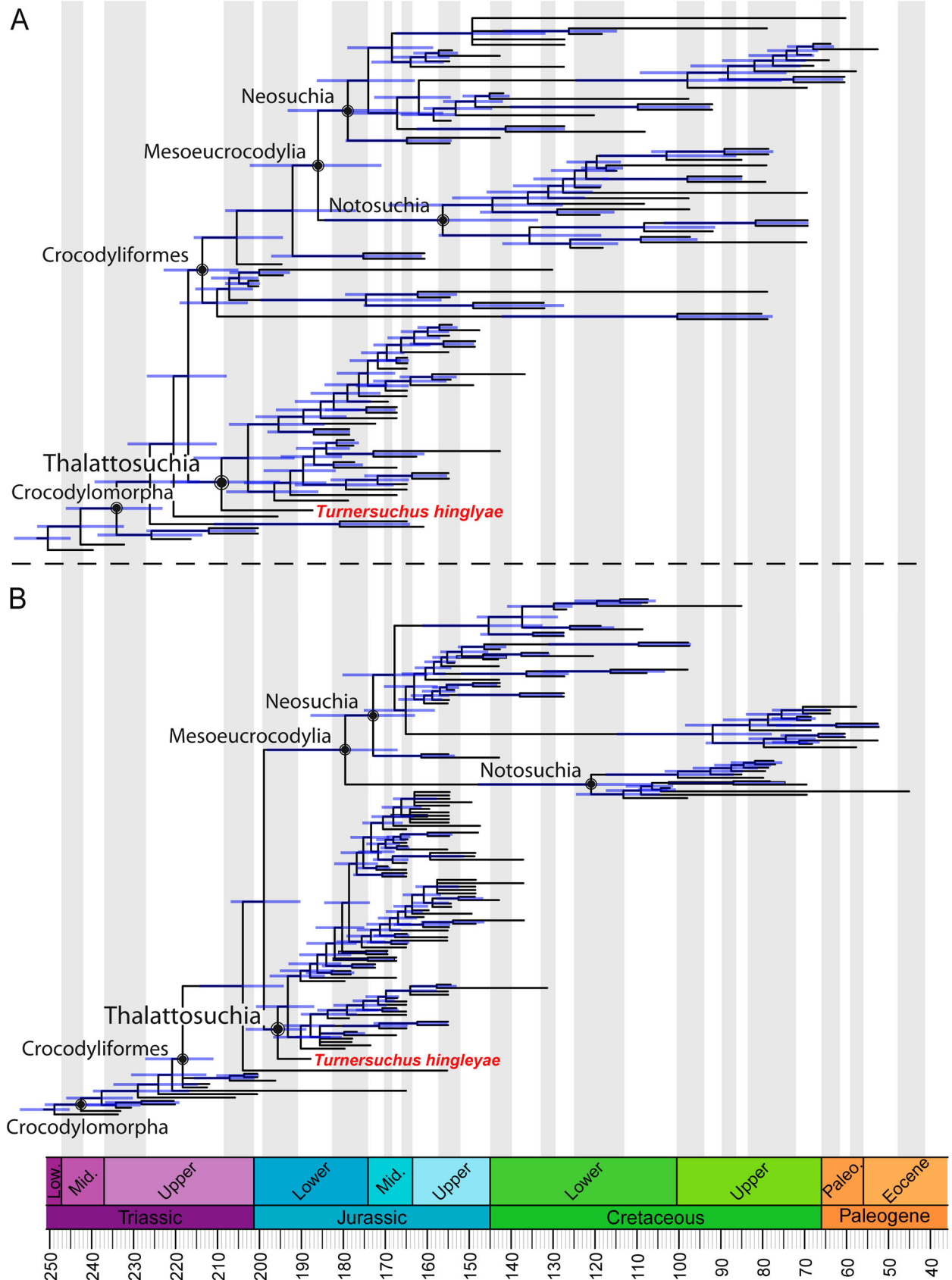


FIGURE 12. Results of the Bayesian time-calibration analyses (95% HPD age ranges for each node indicated by horizontal bars). For visualization purposes, Crocodylia is omitted in both trees, even though representatives of the group were included in the analyses. **A.** time-scaled strict consensus resulting from analysis of the dataset based on Wilberg et al. (2019); **B.** time-scaled strict consensus resulting from analysis of the dataset based on Herrera et al. (2021) with the position of *Eopneumatosuchus* manually changed to fall within Protosuchia.

quadrate articulates with the a broadly exposed prootic, but lacks a contact with the laterosphenoid or parietal. The pterygoid process of the quadrate has a relatively short suture with the pterygoid ventrally, and a more dorsally positioned orbital process that projects along the lateral wall of the braincase but does not suture to the adjacent bones. In other thalattosuchians (e.g., *Pelagosaurus*, *Macrospondylus*, *Teleosaurus*, *Cricosaurus*), this orbital process projects anterior to the trigeminal foramen, forming part of the floor of the trigeminal fossa. The orbital process of *Turnersuchus* is shorter than that of *Pelagosaurus* (NHMUK PV OR 32599; Holliday & Witmer, 2009), ending well posterior to the trigeminal foramen (Fig. 3A, B). It is likely that the slight disarticulation of the bones of the braincase has exaggerated this feature, but it still seems doubtful the orbital process would have reached this far anteriorly. This demonstrates that the quadrate of *Turnersuchus* is less integrated into the lateral wall of the braincase than in crocodyliforms, or even in later diverging thalattosuchians.

A second feature in which *Turnersuchus* appears more plesiomorphic than later-diverging thalattosuchians relates to the development of the basioccipital tubera. Enlarged basioccipital tubera are not a unique feature of thalattosuchians. Rather, the possession of enlarged tubera have been suggested to correlate with longirostry (Langston, 1973; Clark, 1994; Busbey, 1995; Brochu, 2001; Pol & Gasparini, 2009), likely reflecting modifications to the *M. basioccipitovertebralis* and *M. occipitotransversalis* muscles related to moving an elongate skull with a slender snout. Nearly all thalattosuchians possess highly elongate, slender snouts (Drumheller & Wilberg, 2020), including all previously known early-diverging forms (e.g., *Pelagosaurus*, *Plagiophthalmosuchus*). That *Turnersuchus* possesses poorly developed tubera suggests that it may have possessed a shorter snout than later thalattosuchians and that longirostry may not be the plesiomorphic condition of the clade. The only other thalattosuchian with rather poorly developed basioccipital tubera is *Dakosaurus andiniensis*, which possesses a remarkably short snout (Pol & Gasparini, 2009). While the snout of *Turnersuchus* may not have been as elongate as that of *Pelagosaurus* or *Plagiophthalmosuchus*, the shape of the preserved portion of the anterior dentary indicates that the snout was likely slender, even if not particularly elongated.

Divergence Time of Thalattosuchia

Turnersuchus helps fill in part of the unsampled ghost lineage of Thalattosuchia. However, the time-scaling analyses suggest this lineage continues deeper, though the length of the unsampled time varies depending on the tree topology. If thalattosuchians are early-diverging mesoeucrocodylians (as in the Herrera et al. topology), then the remaining length of this unsampled lineage is short, most likely extending to the Sinemurian. If thalattosuchians are the sister-group to Crocodyliformes (as in the Wilberg et al. topology), then this ghost lineage extends much further, into the Norian (representing a 13.57 Ma difference between the two topologies). The 95% HPD ranges of both topologies include Thalattosuchia origination times in the Late Triassic, although in the Herrera et al. topology the oldest possible age of origination for the group would not exceed the Rhaetian, whereas in the Wilberg et al. topology the maximum age of the 95% HPD range would be 18.13 Ma older, within the Norian.

During the revisions to this manuscript, a new thalattosuchian specimen was published from the Hettangian–Sinemurian of Morocco (Hicham et al., *in press*). This new specimen is assignable to Thalattosuchia. The authors further assign it to Teleosaurioidea indet. based on mandibular, premaxillary, and maxillary characters shared with that group. The new discovery corroborates the predictions made in this work that thalattosuchian

specimens should be found in sediments older than the Pliensbachian and supports a thalattosuchian origin prior to the Hettangian–Sinemurian, likely in the Late Triassic (as predicted in the time-scaling analyses presented here).

Crocodylomorpha is the only pseudosuchian lineage to survive the end-Triassic Mass extinction event (e.g., Brusatte et al., 2008; Stubbs et al., 2013). However, within Crocodylomorpha, multiple individual lineages are inferred to have crossed the Triassic/Jurassic boundary (e.g., Leardi et al., 2017; Turner et al., 2017). Currently, only two crocodyliform species are known from the Triassic: *Hemiprotosuchus leali*, and *Coloradisuchus abelini*—both from Norian deposits in northwestern Argentina (Martínez et al., 2018), providing direct evidence that Protosuchidae crossed the boundary. Our time-scaling analyses also suggest other crocodylomorph lineages, including Thalattosuchia, originated in the Triassic and survived the extinction event (Fig. 12). The survivorship of crocodylomorphs inhabiting different environments (e.g., terrestrial protosuchids and aquatic thalattosuchians) indicates that habitat preference did not play a central role in extinction selectivity of pseudosuchians, in agreement with previous investigations of possible drivers (biotic and abiotic) during the end-Triassic Mass extinction event (Allen et al., 2019).

CONCLUSION

Turnersuchus represents the earliest diagnostic thalattosuchian material known to date. Our phylogenetic analyses recover it as the earliest diverging thalattosuchian. However, this position is supported by only a single unambiguous synapomorphy in each analysis and may change with the addition of new taxa or characters. Morphologically, *Turnersuchus* resembles *Pelagosaurus* and *Plagiophthalmosuchus* in many ways, helping to cement numerous features such as large supratemporal fenestrae, presence of a squamosal facet, broad exposure of the prootic on the lateral braincase wall, and orbital process of the quadrate without bony attachment to the laterosphenoid or parietal as plesiomorphic for the group. Supporting its position as the earliest diverging member of the clade, *Turnersuchus* possesses weakly developed basioccipital tubera and a quadrate less integrated with the braincase relative to other thalattosuchians. Time-scaling analyses recover a Late Triassic–Early Jurassic origin of Thalattosuchia, suggesting that a significant ghost lineage remains.

ACKNOWLEDGMENTS

The authors would like to thank P. Turner and E. Hingley for discovering, excavating, and donating the main blocks of the specimen and K. Turner, E. Thompson, L. Pickering, and L. Fowler for discovering and donating other parts. We thank E. Hingley for preparing the specimen. P. Davidson and the Charmouth Heritage Coast Centre assisted with excavation and uniting the parts. We thank P. Davis (LYMPH) for providing information on the geologic setting and for specimen photographs. We thank T. Davies of the XTM Facility, Palaeobiology Research Group, University of Bristol, for assistance with CT scanning. We thank M. Rabi and C. Brochu for comments that improved the manuscript and D. Schwarz for handling the manuscript. TNT is made freely available through the Willi Hennig Society. EWW, PLG, and AHT were supported by NSF-DEB 1754596. PLG was also supported by Coordenação de Aperfeiçoamento de Pessoal de Nível Superior (CAPES grant number: 88887.583087/2020-00) and the São Paulo Research Foundation (FAPESP grant number: 2022/05697-9).

ORCID

Eric W. Wilberg  <http://orcid.org/0000-0002-7038-0825>

Pedro L. Godoy  <http://orcid.org/0000-0003-4519-5094>
 Roger B. J. Benson  <http://orcid.org/0000-0001-8244-6177>

LITERATURE CITED

- Aiglstorfer, M., Havlik, P., & Herrera, Y. (2020). The first metriorhynchoid crocodyliform from the Aalenian (Middle Jurassic) of Germany, with implications for the evolution of Metriorhynchoidea. *Zoological Journal of the Linnean Society*, 188(2), 522–551. <https://doi.org/10.1093/zoolin/zz072>
- Allen, B. J., Stubbs, T. L., Benton, M. J., & Puttick, M. N. (2019). Archosauromorph extinction selectivity during the Triassic–Jurassic mass extinction. *Palaeontology*, 62(2), 211–224.
- Andrade, M. B. d., Edmonds, R., Benton, M. J., & Schouten, R. (2011). A new Berriasian species of *Goniopholis* (Mesoeucrocodylia, Neosuchia) from England, and a review of the genus. *Zoological Journal of the Linnean Society*, 163, S66–S108.
- Andrews, C. W. (1913). *A descriptive catalogue of the marine reptiles of the Oxford Clay, Part II*. British Museum (Natural History).
- Ballell, A., Moon, B. C., Porro, L. B., Benton, M. J., & Rayfield, E. J. (2019). Convergence and functional evolution of longirostry in crocodylomorphs. *Palaeontology*, 62(6), 867–887. <https://doi.org/10.1111/pala.12432>
- Bapst, D. W. (2012). paleotree: an R package for paleontological and phylogenetic analyses of evolution. *Methods in Ecology and Evolution*, 3, 803–807.
- Barton, C. M., Woods, M. A., Bristow, C., Newall, A., Westhead, R., Evans, D. J. A., Kirkby, G., Warrington, G., Riding, J., & Gibson, A. (2011). *Geology of south Dorset and south-east Devon and its World Heritage Coast: special memoir for 1:50,000 geological sheets 328 Dorchester, 341/342 West Fleet and Weymouth and 342/343 Swanage, and parts of sheets 326/340 Sidmouth, 327 Bridport, 329 Bournemouth and 339 Newton Abbot*. British Geological Survey.
- Benton, M. J., & Clark, J. M. (1988). Archosaur phylogeny and the relationships of the Crocodylia. In *The Phylogeny and Classification of Tetrapods* (Vol. Volume 1: Amphibians, Reptiles, Birds, pp. 295–338). Clarendon Press.
- Benton, M. J., & Taylor, M. A. (1984). Marine reptiles from the Upper Lias (Lower Toarcian, Lower Jurassic) of the Yorkshire coast. *Proceedings of the Yorkshire Geological Society*, 44, 399–429.
- Brochu, C. A. (2001). Crocodylian snouts in space and time: Phylogenetic approaches toward adaptive radiation. *American Zoologist*, 41, 564–585.
- Brochu, C. A., Bouare, M. L., Sissoko, F., Roberts, E. M., & O’Leary, M. A. (2002). A dyrosaurid crocodyliform braincase from Mali. *Journal of Paleontology*, 76(6), 1060–1071.
- Brusatte, S. L., Benton, M. J., Ruta, M., & Lloyd, G. T. (2008). Superiority, competition, and opportunism in the evolutionary radiation of dinosaurs. *Science*, 321(5895), 1485–1488.
- Brusatte, S. L., Muir, A., Young, M. T., Walsh, S., Steel, L., & Witmer, L. M. (2016). The braincase and neurosensory anatomy of an Early Jurassic marine crocodylomorph: implications for crocodylian sinus evolution and sensory transitions. *The Anatomical Record*, 299, 1511–1530. <https://doi.org/10.1002/ar.23462>
- Buffetaut, E. (1980). Position systematique et phylogenetique du genre *Pelagosaurus* Bronn, 1841 (Crocodylia, Mesosuchia), du Toarcian d’Europe. *Geobios*, 13(5), 783–786.
- Buffetaut, E. (1982). Radiation evolutive, paleoecologie et biogeographie des crocodiliens mesosuchiens. *Memoires de la Societe Geologique de France*, 142, 1–88.
- Buffetaut, E., Termier, G., & Termier, H. (1981). A teleosaurid (Crocodylia, Mesosuchia) from the Toarcian of Madagascar and its palaeobiogeographical significance. *Paläontologische Zeitschrift*, 55(3), 313–319.
- Busbey, A. B. (1995). The structural consequences of skull flattening in crocodylians. In J. J. Thomason (Ed.), *Functional Morphology in Vertebrate Paleontology* (pp. 173–192). Cambridge University Press.
- Chong Díaz, G., & Gasparini, Z. (1972). Presencia de Crocodylia marinos en el Jurásico de Chile. *Revista de la Asociación Geológica Argentina*, 27(4), 406–409.
- Clark, J. M. (1986). *Phylogenetic relationships of the crocodylomorph archosaurs* [Dissertation, University of Chicago]. Chicago.
- Clark, J. M. (1994). Patterns of Evolution in Mesozoic Crocodyliformes. In N. C. Fraser & H.-D. Sues (Eds.), *In the Shadow of the Dinosaurs: Early Mesozoic Tetrapods* (pp. 84–97). Cambridge University Press.
- Clark, J. M., Xu, X., Forster, C. A., & Wang, Y. (2004). A Middle Jurassic ‘sphenosuchian’ from China and the origin of the crocodylian skull. *Nature*, 430, 1021–1024.
- Coddington, J., & Scharff, N. (1994). Problems with zero-length branches. *Cladistics*, 10, 415–423.
- Colbert, E. H. (1946). The Eustachian Tubes in the Crocodylia. *Copeia*, 1, 11–14.
- Dollman, K. N., & Choiniere, J. N. (2022). Palate evolution in early-branching crocodylomorphs: Implications for homology, systematics, and ecomorphology. *The Anatomical Record*.
- Drumheller, S. K., & Wilberg, E. W. (2020). A synthetic approach for assessing the interplay of form and function in the crocodyliform snout. *Zoological Journal of the Linnean Society*, 188(2), 507–521.
- Duffin, C. J. (1979). *Pelagosaurus* (Mesosuchia, Crocodylia) from the English Toarcian (Lower Jurassic). *Neues Jahrbuch für Geologie und Paläontologie. Monatshefte*, 1979, 475–485.
- Eudes-Deslongchamps, E. (1863–1869). *Notes Paléontologiques*. Le Blanc-Hardel et Savy.
- Ezcurra, M. D., & Butler, R. J. (2018). The rise of the ruling reptiles and ecosystem recovery from the Permo-Triassic mass extinction. *Proceedings of the Royal Society B*, 285(1880), 20180361.
- Fernández, M. S., Carabajal, A. P., Gasparini, Z., & Chong Díaz, G. (2011). A metriorhynchid crocodyliform braincase from northern Chile. *Journal of Vertebrate Paleontology*, 31(2), 369–377.
- Foffa, D., Young, M. T., Brusatte, S. L., Graham, M. R., & Steel, L. (2018). A new metriorhynchid crocodylomorph from the Oxford Clay Formation (Middle Jurassic) of England, with implications for the origin and diversification of Geosaurini. *Journal of Systematic Palaeontology*, 16(13), 1123–1143. <https://doi.org/10.1080/14772019.2017.1367730>
- Fraas, E. (1901). Die Meerkrokodile (Thalattosuchia ng) eine neue sauriergruppe der Juraformation. *Jahreshefte des Vereins für vaterländische Naturkunde in Württemberg*, 57, 409–418.
- Gasparini, Z., Vignaud, P., & Chong, G. (2000). The Jurassic Thalattosuchia (Crocodyliformes) of Chile: a paleobiogeographic approach. *Bulletin de la Société Géologique de France*, 171(6), 657–664.
- Goloboff, P. A., & Catalano, S. A. (2016). TNT version 1.5, including a full implementation of phylogenetic morphometrics. *Cladistics*, 32(3), 221–238. <https://doi.org/10.1111/cla.12160>
- Hay, O. P. (1930). *Second bibliography and catalogue of the fossil vertebrata of North America*.
- Heath, T. A., Huelsenbeck, J. P., & Stadler, T. (2014). The fossilized birth-death process for coherent calibration of divergence-time estimates. *Proceedings of the National Academy of Sciences*, 11(29), E2957–E2966.
- Herrera, Y. (2015). Metriorhynchidae (Crocodylomorpha, Thalattosuchia) from Upper Jurassic-Lower Cretaceous of Neuquén Basin (Argentina), with comments on the natural casts of the brain. In M. Fernández & Y. Herrera (Eds.), *Reptiles Extintos - Volumen en Homenaje a Zulma Gasparini* (Vol. 15, pp. 159–171). Publicación Electrónica de la Asociación Paleontológica Argentina.
- Herrera, Y., Aiglstorfer, M., & Bronzati, M. (2021). A new species of *Cricosaurus* (Thalattosuchia: Crocodylomorpha) from southern Germany: the first three-dimensionally preserved *Cricosaurus* skull from the Solnhofen Archipelago. *Journal of Systematic Palaeontology*, 19(2), 145–167.
- Herrera, Y., Fernández, M. S., & Gasparini, Z. (2013). Postcranial skeleton of *Cricosaurus araucanensis* (Crocodyliformes: Thalattosuchia): morphology and palaeobiological insights. *Alcheringa: An Australasian Journal of Palaeontology*, 37(3), 285–298. <https://doi.org/10.1080/03115518.2013.743709>
- Herrera, Y., Gasparini, Z., & Fernández, M. S. (2015). *Purranisaurus potens* Rusconi, an enigmatic metriorhynchid from the Late Jurassic-Early Cretaceous of Neuquén Basin. *Journal of Vertebrate Paleontology*, 35(2), e904790. <https://doi.org/10.1080/02724634.2014.904790>
- Herrera, Y., Leardi, J. M., & Fernandez, M. S. (2018). Braincase and endocranial anatomy of two thalattosuchian crocodylomorphs and

- their relevance in understanding their adaptations to the marine environment. *PeerJ*, 6, e5686. <https://doi.org/10.7717/peerj.5686>
- Hicham, B., Nehili, A., Ouzzaoui, L. A., Jouve, S., Boudad, L., Masrour, M., Jalil, N., & Arrad, T. Y. (in press). Discovery of the teleosauroid crocodylomorph from the early Jurassic of Chaara cave, Middle Atlas of Morocco. *Journal of African Earth Sciences*, 104804. <https://doi.org/https://doi.org/10.1016/j.jafrearsci.2022.104804>.
- Holliday, C. M., & Nesbitt, S. J. (2013). Morphology and diversity of the mandibular symphysis of archosauriforms. *Geological Society, London, Special Publications*, 379, 555–571. <https://doi.org/10.1144/SP379.2>
- Holliday, C. M., & Witmer, L. M. (2009). The epipterygoid of crocodyliforms and its significance for the evolution of the orbitotemporal region of eusuchians. *Journal of Vertebrate Paleontology*, 29(3), 715–733.
- Hua, S. (2020). A new specimen of *Teleidosaurus calvadosii* (Eudes-Deslongchamps, 1866) (Crocodylia, Thalattosuchia) from the Middle Jurassic of France. *Annales de Paléontologie*, 106(4), 102423. <https://doi.org/https://doi.org/10.1016/j.annpal.2020.102423>
- Hua, S., & Buffetaut, E. (1997). Part V. Crocodylia. In J. M. Callaway & E. L. Nicholls (Eds.), *Ancient Marine Reptiles* (pp. 357–374). Academic Press.
- Huene, F. v. (1927). Beitrag zur Kenntnis mariner Mesozoischer Wirbeltiere in Argentinien. *Centralblatt für Mineralogie, Geologie und Paläontologie Abteilung B*, 1, 22–29.
- Huene, F. v., & Maubeuge, P. L. (1954). Sur quelques restes de Sauriens du Rhétien et du Jurassique lorrain. *Bulletin de la Société de France, Serie 6*, 4 (1-3), 105–105.
- Jäger, C. F. (1828). *Über die fossile Reptilien, welche in Württemberg aufgefunden worden sind*. J. B. Metzler.
- Johnson, M. M., Young, M. T., & Brusatte, S. L. (2020a). Emptying the wastebasket: a historical and taxonomic revision of the Jurassic crocodylomorph *Steneosaurus*. *Zoological Journal of the Linnean Society*, 189(2), 428–448. <https://doi.org/10.1093/zoolinnean/zlaa027>
- Johnson, M. M., Young, M. T., & Brusatte, S. L. (2020b). The phylogenetics of Teleosauroidea (Crocodylomorpha, Thalattosuchia) and implications for their ecology and evolution. *PeerJ*, 8(e9808), 1–157. <https://doi.org/10.7717/peerj.9808>
- Johnson, M. M., Young, M. T., Steel, L., Foffa, D., Smith, A. S., Hua, S., Havlik, P., Howlett, E. A., & Dyke, G. J. (2017). Re-description of ‘*Steneosaurus obtusidens* Andrews, 1909, an unusual macrophagous teleosauroid crocodylomorph from the Middle Jurassic of England. *Zoological Journal of the Linnean Society*, 182, 385–418. <https://doi.org/10.1093/zoolinnean/zlx035>
- Jouve, S. (2009). The skull of *Teleosaurus cadomensis* (Crocodylomorpha; Thalattosuchia), and phylogenetic analysis of Thalattosuchia. *Journal of Vertebrate Paleontology*, 29(1), 88–102.
- Jouve, S., Iarochéne, M., Bouya, B., & Amaghaz, M. (2006). A new species of *Dyrosaurus* (Crocodylomorpha, Dyrosauridae) from the early Eocene of Morocco: phylogenetic implications. *Zoological Journal of the Linnean Society*, 148, 603–656.
- xLang, W. D., Spath, L. F., Cox, L. R., & Muir-Wood, H. M. (1928). The Belemnite Marls of Charmouth, a series in the Lias of the Dorset Coast. *Quarterly Journal of the Geological Society*, 84(1-4), 179–222.
- Langston, W., Jr. (1973). The crocodylian skull in historical perspective. In C. Gans & T. Parsons (Eds.), *Biology of the Reptilia* (Vol. 4, pp. 263–284). Academic Press.
- Larsson, H. C. E., & Sues, H.-D. (2007). Cranial osteology and phylogenetic relationships of *Hamadasuchus rebouli* (Crocodyliformes: Mesoeucrocodylia) from the Cretaceous of Morocco. *Zoological Journal of the Linnean Society*, 149, 533–567.
- Leardi, J. M., Fiorelli, L. E., & Gasparini, Z. (2015). Redescription and reevaluation of the taxonomical status of *Microsaurus schilleri* (Crocodyliformes: Mesoeucrocodylia) from the Upper Cretaceous of Neuquén, Argentina. *Cretaceous Research*, 52, 153–166.
- Leardi, J. M., Pol, D., & Clark, J. M. (2017). Detailed anatomy of the braincase of *Macelognathus vagans* Marsh, 1884 (Archosauria, Crocodylomorpha) using high resolution tomography and new insights on basal crocodylomorph phylogeny. *PeerJ*, 5, e2801. <https://doi.org/10.7717/peerj.2801>
- Leardi, J. M., Pol, D., & Clark, J. M. (2020). Braincase anatomy of *Almadasuchus figarii* (Archosauria, Crocodylomorpha) and a review of the cranial pneumaticity in the origins of Crocodylomorpha. *Journal of Anatomy*, 237(1), 48–73. <https://doi.org/10.1111/joa.13171>
- Li, J. (1993). A new specimen of *Peipehsuchus teleorhinus* from Ziliujing Formation of Daxian, Sichuan. *Vertebrata Palasiatica*, 85–94.
- Martin, J. E., Suteethorn, S., Lauprasert, K., Tong, H., Buffetaut, E., Liard, R., Salaviale, C., Deesri, U., Suteethorn, V., & Claude, J. (2019). A new freshwater teleosauroid from the Jurassic of northeastern Thailand. *Journal of Vertebrate Paleontology*, 38, e1549059. <https://doi.org/10.1080/02724634.2018.1549059>
- Martínez, R. N., Alcober, O. A., & Pol, D. (2018). A new protosuchid crocodyliform (Pseudosuchia, Crocodylomorpha) from the Norian Los Colorados Formation, northwestern Argentina. *Journal of Vertebrate Paleontology*, 38(4), (1)–(12). <https://doi.org/10.1080/02724634.2018.1491047>
- Matzke, N. J., & Wright, A. (2016). Inferring node dates from tip dates in fossil Canidae: the importance of tree priors. *Biology Letters*, 12(8), 20160328.
- Melstrom, K. M., Turner, A. H., & Irmis, R. B. (2022). Reevaluation of the cranial osteology and phylogenetic position of the early crocodyliform *Eopneumatosuchus colberti*, with an emphasis on its endocranial anatomy. *The Anatomical Record*, 305(n10), 2557–2582. <https://doi.org/https://doi.org/10.1002/ar.24777>
- Montefeltro, F. C., Larsson, H. C. E., de França, M. A. G., & Langer, M. C. (2013). A new neosuchian with Asian affinities for the Jurassic of northeastern Brazil. *Naturwissenschaften*, 100, 835–841.
- Mook, C. C. (1921). Notes on the postcranial skeleton in the Crocodylia. *Bulletin of the American Museum of Natural History*, 44, 67–100.
- Mueller-Töwe, I. J. (2006). *Anatomy, phylogeny, and paleoecology of the basal thalattosuchians (Mesoeucrocodylia) from the Liassic of Central Europe* [PhD, Johannes Gutenberg-Universität Mainz].
- Nesbitt, S. J. (2011). The early evolution of archosaurs: relationships and the origin of major clades. *Bulletin of the American Museum of Natural History*, 352, 1–292.
- O’Leary, M. A., & Kaufman, S. (2011). MorphoBank: phylophenomics in the “cloud”. *Cladistics*, 27(5), 529–537.
- O’Leary, M. A., & Kaufman, S. (2012). *MorphoBank 3.0: Web application for morphological phylogenetics and taxonomy*. <http://www.morphobank.org>
- Ósi, A., Young, M. T., Galász, A., & Rabi, M. (2018). A new large-bodied thalattosuchian crocodyliform from the Lower Jurassic (Toarcian) of Hungary, with further evidence of the mosaic acquisition of marine adaptations in Metriorhynchoidea. *PeerJ*, 6, e4668. <https://doi.org/10.7717/peerj.4668>
- Owen, R. (1852). Note on the crocodylian remains accompanying Dr. T. L. Bell’s paper on Kotah. *Quarterly Journal of the Geological Society of London*, 8, 233–234.
- Page, K. N. (2010). Stratigraphical framework. In A. R. Lord & P. G. Davis (Eds.), *Fossils from the Lower Lias of the Dorset Coast* (pp. 33–53). The Palaeontological Association.
- Pierce, S. E., Angielczyk, K., & Rayfield, E. J. (2009a). Morphospace occupation in thalattosuchian crocodylomorphs: skull shape variation, species delineation and temporal patterns. *Palaentology*, 52, 1057–1097.
- Pierce, S. E., Angielczyk, K. D., & Rayfield, E. J. (2009b). Shape and mechanics in thalattosuchian (Crocodylomorpha) skulls: implications for feeding behaviour and niche partitioning. *Journal of Anatomy*, 215(5), 555–576.
- Pierce, S. E., & Benton, M. J. (2006). *Pelagosaurus typus* Bronn, 1841 (Mesoeucrocodylia: Thalattosuchia) from the Upper Lias (Toarcian, Lower Jurassic) of Somerset, England. *Journal of Vertebrate Paleontology*, 26(3), 621–635.
- Pol, D. (2005). Postcranial remains of *Notosuchus terrestris* (Archosauria: Crocodyliformes) from the upper Cretaceous of Patagonia, Argentina. *Ameghiniana*, 42, 21–38.
- Pol, D., & Gasparini, Z. (2007). Crocodyliformes. In Z. Gasparini, L. Salgado, & R. A. Coria (Eds.), *Patagonian Mesozoic Reptiles* (pp. 116–142). Indiana University Press.
- Pol, D., & Gasparini, Z. (2009). Skull anatomy of *Dakosaurus andiniensis* (Thalattosuchia: Crocodylomorpha) and the phylogenetic position of Thalattosuchia. *Journal of Systematic Palaeontology*, 7(2), 163–197.
- Pol, D., Nascimento, P. M., Carvalho, A. B., Riccomini, C., Pires-Domingues, R. A., & Zaher, H. (2014). A new notosuchian from the Late Cretaceous of Brazil and the phylogeny of advanced notosuchians. *PLoS One*, 9(4), e93105.

- Pol, D., Rauhut, O. W. M., Leucona, A., Leardi, J. M., Xu, X., & Clark, J. M. (2013). A new fossil from the Jurassic of Patagonia reveals the early basicranial evolution and the origins of Crocodyliformes. *Biological Reviews*, 88, 862–872. <https://doi.org/10.1111/brv.12030>
- Ristevski, J., Young, M. T., De Andrade, M. B., & Hastings, A. K. (2018). A new species of Anteophthalmosuchus (Crocodylomorpha, Goniopholididae) from the Lower Cretaceous of the Isle of Wight, United Kingdom, and a review of the genus. *Cretaceous Research*, 84, 340–383.
- Ronquist, F., Klopfstein, S., Vilhelmsen, L., Schulmeister, S., Murray, D. L., & Rasnitsyn, A. P. (2012a). A total-evidence approach to dating with fossils, applied to the early radiation of the Hymenoptera. *Systematic Biology*, 61, 973–999.
- Ronquist, F., Teslenko, M., van der Mark, P., Ayres, D. L., Darling, A., Höhna, S., Larget, B., Liu, L., Suchard, M. A., & Huelsenbeck, J. P. (2012b). MrBayes 3.2: Efficient Bayesian Phylogenetic Inference and Model Choice Across a Large Model Space. *Systematic Biology*, 61(3), 539–542. <https://doi.org/10.1093/sysbio/sys029>
- Ruebenstahl, A. A., Klein, M. D., Yi, H., Xu, X., & Clark, J. M. (2022). Anatomy and relationships of the early diverging Crocodylomorphs *Junggarsuchus sloani* and *Dibothrosuchus elaphros*. *The Anatomical Record*, n/a(n/a). <https://doi.org/https://doi.org/10.1002/ar.24949>
- Sachs, S., Johnson, M. M., Young, M. T., & Abel, P. (2019). The mystery of *Mystrisaurus* Kaup, 1834: redescribing the poorly known Early Jurassic teleosauroid thalattosuchians *Mystrisaurus laurillardi* Kaup, 1834 and *Stenosaurs brevior* Blake, 1876. *Acta Palaeontologica Polonica*, 64, 565–579.
- Sachs, S., Young, M. T., & Hornung, J. J. (2020). The enigma of *Enaliosuchus*, and a reassessment of the Lower Cretaceous fossil record of Metriorhynchidae. *Cretaceous Research*, 114, 104479.
- Scapino, R. (1981). Morphological investigation into functions of the jaw symphysis in carnivorans. *Journal of Morphology*, 167(3), 339–375.
- Sereno, P. C., & Larsson, H. C. (2009). Cretaceous crocodyliforms from the Sahara. *ZooKeys*, 28, 1–143. <https://doi.org/doi:10.3897/zookeys.28.325>
- Sereno, P. C., Larsson, H. C., Sidor, C. A., & Gado, B. (2001). The giant crocodyliform *Sarcosuchus* from the Cretaceous of Africa. *Science*, 294(5546), 1516–1519. <https://doi.org/10.1126/science.1066521>
- Sereno, P. C., Sidor, C. A., Larsson, H. C. E., & Gado, B. (2003). A new notosuchian from the Early Cretaceous of Niger. *Journal of Vertebrate Paleontology*, 23(2), 477–482.
- Stadler, T. (2010). Sampling-through-time in birth-death trees. *Journal of Theoretical Biology*, 267(3), 396–404.
- Stubbs, T. L., Pierce, S. E., Rayfield, E. J., & Anderson, P. S. (2013). Morphological and biomechanical disparity of crocodile-line archosaurs following the end-Triassic extinction. *Proceedings of the Royal Society B: Biological Sciences*, 280(1770), 20131940.
- Turner, A. H. (2006). Osteology and phylogeny of a new species of *Araripesuchus* (Crocodyliformes: Mesoeucrocodylia) from the Late Cretaceous of Madagascar. *Historical Biology*, 18(3), 255–369.
- Turner, A. H. (2015). A review of *Shamosuchus* and *Paralligator* (Crocodyliformes, Neosuchia) from the Cretaceous of Asia. *PLoS One*, 10(2), e0118116.
- Turner, A. H., & Pritchard, A. C. (2015). The monophyly of Suisuchidae (Crocodyliformes) and its phylogenetic placement in Neosuchia. *PeerJ*, 3. <https://doi.org/10.7717/peerj.759>
- Turner, A. H., Pritchard, A. C., & Matzke, N. J. (2017). Empirical and Bayesian approaches to fossil-only divergence times: A study across three reptile clades. *PLoS One*, 12(2), e0169885. <https://doi.org/10.1371/journal.pone.0169885>
- Turner, A. H., & Sertich, J. J. W. (2010). Phylogenetic history of *Simosuchus clarki* (Crocodyliformes: Notosuchia) from the Late Cretaceous of Madagascar. *Journal of Vertebrate Paleontology*, 30(6), 177–236.
- Tykoski, R. S., Rowe, T., Ketcham, R. A., & Colbert, M. W. (2002). *Calsoyasuchus valliceps*, a new crocodyliform from the Early Jurassic Kayenta Formation of Arizona. *Journal of Vertebrate Paleontology*, 22(3), 593–611.
- Vignaud, P. (1995). *Les Thalattosuchia, crocodiles marins du Mésozoïc: systématique phylogénétique, paléocécologie, biochronologie et implications paléogéographiques* Université de Poitiers]. Poitiers, France.
- Walker, A. D. (1972). New light on the origin of birds and crocodiles. *Nature*, 237, 257–263.
- Walker, A. D. (1990). A revision of *Sphenosuchus acutus* Houghton, a crocodylomorph reptile from the Elliot Formation (late Triassic or early Jurassic) of South Africa. *Philosophical Transactions of the Royal Society of London, Series B: Biological Sciences*, 330(1256), 1–120.
- Westphal, F. (1961). Zur Systematik der deutschen und englischen Lias-Krokodilier. *Neues Jahrbuch für Geologie und Paläontologie. Abhandlungen*, 113, 207–218.
- Westphal, F. (1962). Die Krokodilier des deutschen und englischen oberen Lias. *Palaeontographica Abt. A.*, 116, 23–118.
- Wilberg, E. W. (2015a). A new metriorhynchoid (Crocodylomorpha, Thalattosuchia) from the Middle Jurassic of Oregon and the evolutionary timing of marine adaptations in thalattosuchian crocodylomorphs. *Journal of Vertebrate Paleontology*, 35(2), e902846. <https://doi.org/10.1080/02724634.2014.902846>
- Wilberg, E. W. (2015b). What's in an outgroup? The impact of outgroup choice on the phylogenetic position of Thalattosuchia (Crocodylomorpha) and the origin of Crocodyliformes. *Systematic Biology*, 64(4), 621–637. <https://doi.org/10.1093/sysbio/syv020>
- Wilberg, E. W. (2017). Investigating patterns of crocodyliform cranial disparity through the Mesozoic and Cenozoic. *Zoological Journal of the Linnean Society*, 181(1), 189–208. <https://doi.org/https://doi.org/10.1093/zoolinnean/zw027>
- Wilberg, E. W., Beyl, A. R., Pierce, S. E., & Turner, A. H. (2022). Cranial and endocranial anatomy of a three-dimensionally preserved teleosauroid thalattosuchian skull. *The Anatomical Record*, 305(10), 2620–2653. <https://doi.org/https://doi.org/10.1002/ar.24704>
- Wilberg, E. W., Turner, A. H., & Brochu, C. A. (2019). Evolutionary structure and timing of major habitat shifts in Crocodylomorpha. *Scientific Reports*, 9, 514. <https://doi.org/DOI:10.1038/s41598-018-36795-1>
- Wilkinson, L. E., Young, M. T., & Benton, M. J. (2008). A New Metriorhynchid Crocodylian (Mesoeucrocodylia: Thalattosuchia) from the Kimmeridgian (Upper Jurassic) of Wiltshire, UK. *Palaeontology*, 51(6), 1307–1333. <https://doi.org/10.1111/j.1475-4983.2008.00818.x>
- Wu, X.-C., & Chatterjee, S. (1993). *Dibothrosuchus elaphros*, a crocodylomorph from the Lower Jurassic of China and the phylogeny of the Sphenosuchia. *Journal of Vertebrate Paleontology*, 13(1), 58–89.
- Wu, X.-C., Russell, A. P., & Cumbaa, S. L. (2001). *Terminonaris* (Archosauria: Crocodyliformes): new material from Saskatchewan, Canada, and comments on its phylogenetic relationships. *Journal of Vertebrate Paleontology*, 21(3), 492–514.
- Wu, X.-C., Sues, H.-D., & Dong, Z.-M. (1997). *Sichuanosuchus shuhanensis*, a new ?Early Cretaceous protosuchian (Archosauria: Crocodyliformes) from Sichuan (China), and the monophyly of Protosuchia. *Journal of Vertebrate Paleontology*, 17(1), 89–103.
- Young, M. T., & Andrade, M. B. d. (2009). What is *Geosaurus*? Redescription of *Geosaurus giganteus* (Thalattosuchia: Metriorhynchidae) from the Upper Jurassic of Bayern, Germany. *Zoological Journal of the Linnean Society*, 157, 551–585.
- Young, M. T., Andrade, M. B. d., Etches, S., & Beatty, B. L. (2013). A new metriorhynchid crocodylomorph from the Lower Kimmeridge Clay Formation (Late Jurassic) of England, with implications for the evolution of dermatocranium ornamentation in Geosaurini. *Zoological Journal of the Linnean Society*, 169, 820–848.
- Young, M. T., Brignon, A., Sachs, S., Hornung, J. J., Foffa, D., Kitson, J. J. N., Johnson, M. M., & Steel, L. (2021). Cutting the Gordian knot: a historical and taxonomic revision of the Jurassic crocodylomorph Metriorhynchus. *Zoological Journal of the Linnean Society*, 192(2), 510–553. <https://doi.org/10.1093/zoolinnean/zlaa092>
- Young, M. T., Brusatte, S. L., Andrade, M. B. d., Desojo, J. B., Beatty, B. L., Steel, L., Fernandez, M. S., Sakamoto, M., Ruiz-Omenaca, J. I., & Schoch, R. R. (2012). The cranial osteology and feeding ecology of the metriorhynchid crocodylomorph genera *Dakosaurus* and *Plesiosuchus* from the late Jurassic of Europe.

- PLoS One*, 7(9), e44985. <https://doi.org/10.1371/journal.pone.0044985>
- Young, M. T., Brusatte, S. L., Ruta, M., & Andrade, M. B. d. (2010). The evolution of Metriorhynchoidea (Mesoeucrocodylia, Thalattosuchia): an integrated approach using geometric morphometrics, analysis of disparity, and biomechanics. *Zoological Journal of the Linnean Society*, 158, 801–859.
- Young, M. T., Hastings, A. K., Allain, R., & Smith, T. J. (2017). Revision of the enigmatic crocodyliform *Elosuchus felixi* de Lapparent de Broin, 2002 from the Lower-Upper Cretaceous boundary of Niger: potential evidence for an early origin of the clade Dyrosauridae. *Zoological Journal of the Linnean Society*. <https://doi.org/10.1111/zoj.12452>
- Young, M. T., Sachs, S., Abel, P., Foffa, D., Herrera, Y., & Kitson, J. J. (2020). Convergent evolution and possible constraint in the posterodorsal retraction of the external nares in pelagic crocodylomorphs. *Zoological Journal of the Linnean Society*, 189(2), 494–520.
- Zhang, C., Stadler, T., Klopstein, S., Heath, T. A., & Ronquist, F. (2016). Total-evidence dating under the fossilized birth–death process. *Systematic Biology*, 65(2), 228–249.

Submitted July 27, 2022; revisions received December 7, 2022; accepted December 7, 2022; first published online January 20, 2023.
Handling Editor: Daniela Schwarz.
Phylogenetics Editor: Pedro Godoy.